

Orbifold Riemann surfaces and geodesic algebras

L. O. Chekhov¹

*Steklov Mathematical Institute, Moscow, Russia,
Institute for Theoretical and Experimental Physics, Moscow, Russia,
Poncelet Laboratoire International Franco–Russe, Moscow, Russia.*

To the memory of Alesha Zamolodchikov

We study the Teichmüller theory of Riemann surfaces with orbifold points of order two using the fat graph technique. The previously developed technique of quantization, classical and quantum mapping-class group transformations, and Poisson and quantum algebras of geodesic functions is applicable to the surfaces with orbifold points. We describe classical and quantum braid group relations for particular sets of geodesic functions corresponding to A_n and D_n algebras and describe their central elements for the Poisson and quantum algebras.

1 Introduction

Algebraic structures that arise in studies of Teichmüller spaces are an interesting object deserving a deeper investigation and understanding. Particular cases of these algebras happen to be related to algebras of monodromies in Fuchsian systems [9, 25] and to algebras of groupoid of upper triangular matrices [2]. In this paper, we review these cases and present another case of these (closed) Poisson algebras [3]. We also present a new result obtained in collaboration with M. Mazzocco (see [7]) concerning constructing central elements for this new algebra.

Teichmüller spaces of hyperbolic structures on Riemann surfaces admit a fruitful graph (combinatorial) descriptions [22, 12]. These structures proved to be especially useful when describing sets of geodesic functions and the related Poisson and quantum structures [5]. These Riemann surfaces necessarily contain holes. A generalization of this construction to bordered Riemann surfaces [20, 15, 14, 3], or to the Riemann surfaces with \mathbb{Z}_2 -orbifold points [4] was developed. First, Kaufmann and Penner [20] have demonstrated the relation between the Thurston theory of measured foliations and a combinatorial description of open/closed string diagrammatic. The original description in terms of the Teichmüller space coordinates was proposed in [14] for the *ciliated* Riemann surfaces (a *cilium* was there a marked point on the boundary). The algebraic structures behind this geometry

¹E-mail: chekhov@mi.ras.ru.

are cluster algebras (originated in [16] and applied to bordered surfaces in [15]). Then, the Teichmüller theory of bordered surfaces in the shear-coordinate pattern was reconstructed and the corresponding algebras of geodesic functions were investigated in [3].

In [4], we gave a detailed geometrical accounting for the orbifold Riemann surfaces in the graph description; in the present paper, we briefly recall this description, but our main goal is to describe algebras of geodesic functions, the mapping class group transformations, and the corresponding braid group transformations on the level of these algebras (classical and quantum) and to obtain central elements of these algebras in the special cases of algebras of A_n and D_n types.

Riemann surfaces obtained as quotients of the hyperbolic upper half-plane under the action of a Fuchsian subgroup of $PSL(2, \mathbb{R})$ with elliptic elements e_i of a fixed order m_i ($e_i^{m_i} = 1$) (a crystallographic subgroup) has been studied for long (see, e.g., [10] and the references therein). A class of Fuchsian groups generated by half-turns (with all $m_i = 2$) was of a special importance, and a difficult problem was to characterize moduli spaces of such surfaces. It was shown in [4] that the fat graph description provides such a characterization.

In Section 2, we first recall the structure of geodesic functions in the fat graph technique for the Riemann surfaces with holes but without orbifold points. A fat graph is a nondirected graph with marking on the edges and with a prescribed cyclic order of edges entering each vertex. We call a fat graph a *spine* of the corresponding Riemann surface with holes if we can draw this graph without self intersections on this surface and cutting along all the edges of the graph decomposes the surface into a disjoint set of faces: each face contains exactly one hole and becomes simply connected polygon upon gluing this hole.

We then generalize this structures to the case of \mathbb{Z}_2 -orbifold points (half-turns) using that (see [4]) the space of all regular (metrizable) Riemann surfaces with $|\delta|$ \mathbb{Z}_2 -orbifold points is covered by the Teichmüller space of fat graphs with real parameters Z_α on edges and with one- and three-valent vertices; the number of one-valent vertices (endpoints of “pending edges”) is $|\delta|$ whereas the total number of edges is $6g - 6 + 3s + 2|\delta|$ and it coincides with the dimension of the corresponding Teichmüller space. Our main examples are the genus zero Riemann surface with n \mathbb{Z}_2 -orbifold points and *one* hole, which corresponds to the case of A_n algebra, and the genus zero Riemann surface with n \mathbb{Z}_2 -orbifold points and *two* holes (the annulus), which corresponds to the case of D_n algebra [3].

In Section 3 we recall the Poisson brackets for coordinates of the Teichmüller space [14], [3]. We then consider all possible mapping class group transformations generated by flips of edges (internal and pending) of the spine graph and by changing the directions of spiraling to the hole perimeters for lines of an ideal triangle decomposition of the Riemann surface. We prove the invariance of both the set of the geodesic functions and their Poisson relations (the Goldman bracket [17]) under all these transformations thus proving that *any* choice of the spine with *arbitrary* marking of edges provides the same geodesic algebra.

In Section 4, we first describe the Poisson algebras of geodesic functions in the A_n and D_n cases, then present the braid-group transformations that generate the whole group of modular transformations in the A_n and D_n cases and leaves these Poisson algebras invariant and, third, describe the central elements of these two algebras (A_n and D_n).

These are the main results of this paper.

We quantize in Section 5. We briefly recall the quantization procedure from [5] coming then to the quantum geodesic operators and to the corresponding quantum geodesic algebras of A_n and D_n type. We also describe the quantum counterparts of the braid group transformations and the corresponding representations for quantum geodesic functions in the A_n and D_n cases.

2 Graph description and hyperbolic geometry

2.1 Hyperbolic geometry and inversions

2.1.1 Graph description for Riemann surfaces with holes

Recall the fat graph combinatorial description of the Fuchsian group $\Delta_{g,s}$, which is a discrete finitely generated subgroup of $PSL(2, \mathbb{R})$. In the case without orbifold points, we assume a fat graph to be a three-valent graph (each vertex is incident to three terminal points of nonoriented edges; two terminal points of the same edge can be incident to the same vertex) with edges labeled by distinct integers $\alpha = 1, 2, \dots, 6g - 6 + 3s$ and with the prescribed cyclic ordering of edges entering each vertex. A natural way to represent such a graph is to draw it without self-intersections on an orientable Riemann surface with holes.

Definition 1 We call a three-valent fat graph $\Gamma_{g,s}$ a *spine* of the Riemann surface $\Sigma_{g,s}$ of genus g with s holes ($s \geq 1, 2g - 2 + s > 0$) if the fat graph $\Gamma_{g,s}$ can be embed without self-intersections into this Riemann surface in such a way that the complement of a graph is a disjoint set of *faces*, each face being a polygon with exactly one hole inside and gluing this hole makes the face simply-connected.

We consider a spine $\Gamma_{g,s}$ corresponding to the Riemann surface $\Sigma_{g,s}$ with g handles and s boundary components (holes). The first homotopy groups $\pi_1(\Sigma_{g,s})$ and $\pi_1(\Gamma_{g,s})$ coincide because each closed path in $\Sigma_{g,s}$ can be homotopically transformed to a closed path in $\Gamma_{g,s}$ in a unique way. The standard statement in hyperbolic geometry is that conjugate classes of elements of a Fuchsian group $\Delta_{g,s}$ are in the 1-1 correspondence with homotopy classes of closed paths in the Riemann surface $\Sigma_{g,s} = \mathbb{H}_+^2 / \Delta_{g,s}$ and that the “actual” length ℓ_γ of a hyperbolic element $\gamma \in \Delta_{g,s}$ coincides with the minimum length of curves from the corresponding homotopy class: it is then the length of a unique closed geodesic line belonging to this class.

The standard set of generators of the first homotopy group $\pi_1(\Sigma_{g,s})$ comprises $2g$ elements $A_i, B_i, i = 1, \dots, g$, corresponding to going around cycles a_i, b_i in the Riemann surface (with the standard intersection conditions $a_i \circ b_j = \delta_{ij}, a_i \circ a_j = b_i \circ b_j = 0$) and s generators $P_j, j = 1, \dots, s$, corresponding to going around holes (in one and the same direction w.r.t. the orientation of the Riemann surface) with a single restriction that

$$A_1 B_1 A_1^{-1} B_1^{-1} A_2 B_2 A_2^{-1} B_2^{-1} \dots A_g B_g A_g^{-1} B_g^{-1} P_1 \dots P_s = I,$$

from which the total number of parameters is $6g + 3s - 6$ (three parameters fixed by the constraint and three extra fixed by the general conjugation freedom).

The combinatorial description of moduli spaces uses the above 1-1 correspondence between conjugacy classes of the Fuchsian group and closed paths in the spine. We set the real number Z_α into the correspondence to the edge with the label α and insert [12] the matrix of the Möbius transformation

$$X_{Z_\alpha} = \begin{pmatrix} 0 & -e^{Z_\alpha/2} \\ e^{-Z_\alpha/2} & 0 \end{pmatrix} \quad (2.1)$$

each time the path homeomorphic to a geodesic γ passes through the α th edge.

We also introduce the “right” and “left” turn matrices to be set in the proper place when a path makes the corresponding turn,

$$R = \begin{pmatrix} 1 & 1 \\ -1 & 0 \end{pmatrix}, \quad L = R^2 = \begin{pmatrix} 0 & 1 \\ -1 & -1 \end{pmatrix}, \quad (2.2)$$

and define the related operators R_Z and L_Z ,

$$R_Z \equiv RX_Z = \begin{pmatrix} e^{-Z/2} & -e^{Z/2} \\ 0 & e^{Z/2} \end{pmatrix}, \quad (2.3)$$

$$L_Z \equiv LX_Z = \begin{pmatrix} e^{-Z/2} & 0 \\ -e^{-Z/2} & e^{Z/2} \end{pmatrix}. \quad (2.4)$$

An element of a Fuchsian group has then the structure

$$P_\gamma = LX_{Z_n}RX_{Z_{n-1}} \cdots RX_{Z_2}RX_{Z_1},$$

and the corresponding *geodesic function*

$$G_\gamma \equiv \text{tr } P_\gamma = 2 \cosh(\ell_\gamma/2) \quad (2.5)$$

is expressed via the actual length ℓ_γ of the closed geodesic on the Riemann surface.

The total number of parameters here equals the number of edges of $\Gamma_{g,s}$, which, by the Euler formula, is exactly the desired number $6g - 6 + 3s$.

2.1.2 Generalization to surfaces with \mathbb{Z}_2 orbifold points

New generators of the Fuchsian group are rotations through the angle π at a finite set δ of points on the Riemann surface.¹ All these generators F_i , $i = 1, \dots, |\delta|$, are conjugates of the same matrix

$$F_i = U_i F U_i^{-1}, \quad F = \begin{pmatrix} 0 & 1 \\ -1 & 0 \end{pmatrix}. \quad (2.6)$$

Adding this set of generators to the standard one (translations along A - and B -cycles and around holes) not necessarily result in a regular (metrizable) surface because the action

¹We let $|\cdot|$ denote the cardinality of a set.

of the resulting group is not necessarily discrete. The necessary and sufficient conditions for this generators to result in a *regular* surface can be formulated in terms of graphs [4].²

We now extend the notion of the fat graph to the case of orbifold Riemann surfaces. First, we label all the orbifold points by distinct integers $\beta = 1, \dots, n$. Second, we arbitrarily split the set of orbifold points δ into s nonintersecting (may be empty) subsets δ_k , $|\delta_k| \geq 0$, $\cup_{k=1}^s \delta_k = \delta$, and we then associate (in the set-theoretical sense) the k th hole to the subset δ_k . We also introduce the cyclic ordering in every subset δ_k .

Definition 2 We call a fat graph $\Gamma_{g,s,|\delta|}$ a spine of the Riemann surface $\Sigma_{g,s,\delta}$ with g handles, s holes, and $|\delta|$ \mathbb{Z}_2 -orbifold points if

- (a) this graph can be embed without self-intersections in $\Sigma_{g,s,\delta}$,
- (b) all vertices of $\Gamma_{g,s,|\delta|}$ are three-valent except exactly $|\delta|$ one-valent vertices (endpoints of “pending” edges), which are placed at the corresponding orbifold points,
- (c) upon cutting along all edges of $\Gamma_{g,s,|\delta|}$ the Riemann surface $\Sigma_{g,s,\delta}$ splits into s polygons each containing exactly one hole and being simply connected upon gluing this hole.

We therefore set into correspondence to each orbifold point the special one-valence vertex (the end of a *pending edge*) indicated by a dot in figures below.

We now construct a spine $\Gamma_{g,s,|\delta|}$ that represents the above splitting of δ into δ_k . For this, note that every pending edge terminates at an orbifold point belonging to some subset δ_k and points towards some boundary component (hole) (see Fig. 1 and the example in Fig. 6). The spine $\Gamma_{g,s,|\delta|}$ must be such that this is just the hole associated with the set δ_k . A natural w.r.t. the surface orientation cyclic ordering of pending vertices of the spine $\Gamma_{g,s,|\delta|}$ associated to the k th boundary component must coincide with the prescribed cyclic ordering in the subset δ_k .

As the result, we obtain a fat graph of a given genus, a given number of holes (punctures), and a given number of pending edges. We now endow *each* edge of this graph including the pending edges (the total number of edges is $6g - 6 + 3s + 2|\delta|$) with the real number Z_α (the subscript α enumerates the edges of the graph). This pattern was first proposed by Fock and Goncharov [14].

2.1.3 Geodesic functions for Riemann surfaces with \mathbb{Z}_2 orbifold points

There exists a convenient parametrization of the geodesic lines corresponding to elements of the group generated by the complete set of generators. A geodesic line undergoes the *inversion* when it goes around the dot-vertex: we then insert the matrix F (2.6) into the corresponding string of 2×2 -matrices. For example, a part of geodesic function in Fig. 1 that is inverted reads

$$\dots X_{Y_1} L X_Z F X_Z L X_{Y_2} \dots ,$$

²In what follows, we call a Riemann surface regular if it is locally a smooth constant-curvature surface everywhere except exactly $|\delta|$ \mathbb{Z}_2 -orbifold points.

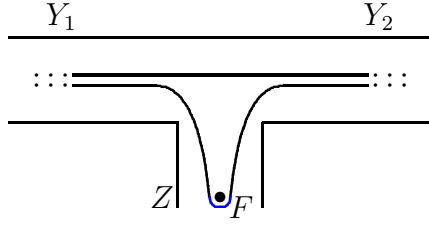


Figure 1: Part of the graph with the pending edge. Its endpoint with the orbifold point is directed to the interior of the boundary component this point is associated with. The variable Z corresponds to the respective pending edge. Two types of geodesic lines are shown in the figure: one that does not come to the edge Z is parameterized in the standard way, the other undergoes the inversion with the matrix F (2.6). The corresponding geodesic line then goes around the dot vertex representing the orbifold point.

whereas the other geodesic that does not go around the dot vertex reads merely

$$\dots X_{Y_1} R X_{Y_2} \dots$$

Note the simple relation,

$$X_Z F X_Z = X_{2Z}. \quad (2.7)$$

Together with the explicit form of R_Z and L_Z (formulas (2.3) and (2.4)), Eq. (2.7) implies that *any* product of R_Z and L_Z (represented by a matrix $\begin{pmatrix} a & b \\ c & d \end{pmatrix}$) always has strictly positive elements on the main diagonal and nonpositive elements on the antidiagonal and, since it has the unit determinant $ad - bc = 1$, its trace $a + d \geq 2$, that is, such an element is almost always hyperbolic; it may be parabolic only when either $b = 0$ or $c = 0$, which happens only when all the matrices in the product are either L_Z or R_Z , and this corresponds to passing around a hole (puncture), and even in this case the trace is two only if the hole is actually a puncture. The only elliptic elements are conjugates of F_i ($\text{tr } F_i = 0$).

We have therefore a metrizable Riemann surface for *any* choice of real numbers Z_α , associated to the edges of a spine; the main lemma in [4] states that the converse is also true: *any* metrizable Riemann surface can be obtained this way. So, in what follows, we identify the Teichmüller space of Riemann surfaces with orbifold points with the space $\mathbb{R}^{6g-6+3s+2|\delta|}$ of real parameters on the edges of a spine $\Gamma_{g,s,|\delta|}$.

We also have the statement concerning the polynomiality of geodesic functions.

Proposition 2.1 *All G_γ constructed by (2.5) are Laurent polynomials in e^{Z_i} and $e^{Y_j/2}$ with positive integer coefficients, that is, we have the Laurent property, which holds, e.g., in cluster algebras [16]. Here we let Z_i denote the variables of pending edges and Y_j denote those of internal edges of the graph. All these geodesic functions preserve their polynomial structures upon Whitehead moves on inner edges (Fig. 7) and upon mapping class group transformations in Fig. 8, in (3.4), and in (3.6). All these geodesic functions correspond to hyperbolic elements ($G_\gamma > 2$), the only exception where $G_\gamma = 2$ are paths homotopic to going around holes of zero length (punctures).*

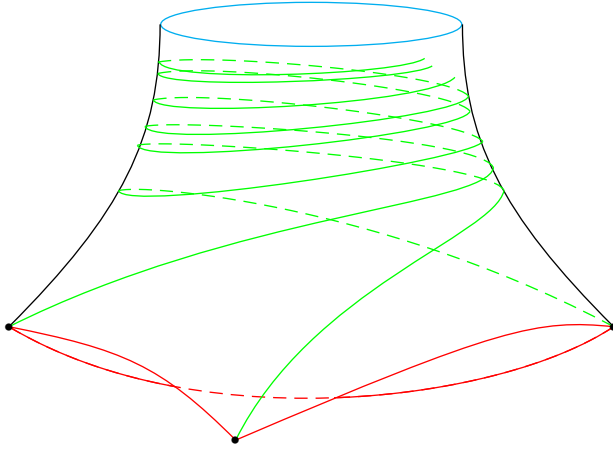


Figure 2: The example of a regular genus zero Riemann surface with three \mathbb{Z}_2 -orbifold points \mathfrak{s}_i and one hole. The orbifold points are connected by finite-length geodesic lines, whereas the geodesic lines of the partition start at the corresponding point \mathfrak{s}_i and spiral asymptotically to the closed geodesic that is the boundary of the hole with the perimeter $\ell_P = |Z_1 + Z_2 + Z_3|$, where Z_i are the Teichmüller space variables (from the graph description).

Example 2.1 For the closed path drawn in Fig. 5, we have

$$\begin{aligned} G_{24} &= \text{tr } L_{Y_2} R_{Y_3} L X_{Z_4} F X_{Z_4} R_{Y_3} L_{Y_2} R X_{Z_2} F X_{Z_2} \\ &= \text{tr } L_{Y_2} R_{Y_3} L_{2Z_4} R_{Y_3} L_{Y_2} R_{2Z_2}. \end{aligned}$$

Before we switch to purely algebraic part of this paper, let us remind the geometric pattern underlying these algebraic constructions. For this, we recall the construction of *ideal triangle decomposition* for orbifold Riemann surfaces.

Given a regular Riemann surface of genus g with s holes and with $|\delta_k|$ \mathbb{Z}_2 -orbifold points assigned to the k th hole and cyclically ordered in every set δ_k , we issue from each of these orbifold points a geodesic line (which is unique in a given homotopy class) that spirals in a given direction (one and the same for all lines spiraling to a given hole) to the perimeter line (the horizon) of this hole. The example of a genus zero Riemann surface with three orbifold points and one hole is depicted in Fig. 2.

For pre-images of the spiraling geodesic lines starting at the orbifold points on the Riemann surface we obtain that, for a \mathbb{Z}_2 -orbifold point, the pre-image of such a line in a Poincaré disc consists of *two half-lines* originating at this point and pointing in opposite directions. We can then represent it as a *single* infinite geodesic line passing through a preimage of the orbifold point. As the result, we have a pattern like the one depicted in Fig. 3, that is, as in the case of Riemann surfaces without orbifold points, the *fundamental domain* is a union of *ideal triangles*. Boundary geodesic curves of this fundamental domain can be of two sorts: either (as in the standard case) an infinite boundary curve is to be identified with another boundary curve of this domain or it contains a unique preimage of a \mathbb{Z}_2 -orbifold point, and we then identify its two halves separated by this point. It follows immediately from this consideration that lines containing preimages of \mathbb{Z}_2 -orbifold points must necessarily lie on the boundary of a fundamental domain.

Note that choosing other representatives of the orbifold points, we obtain different fundamental domains with different cyclic ordering of the (preimages) of the orbifold points s_i ($i = 1, \dots, |\delta_k|$). In Fig. 4 we describe the changing of the fundamental domain when we replace the preimage s_{α_i} by another preimage s'_{α_i} of the same orbifold point obtained upon rotation about the neighbor (in the sense of the natural ordering inherited from the structure of a fundamental domain) point $s_{\alpha_{i+1}}$. As the result, the natural ordering changes: instead of $\{\dots, s_{\alpha_i}, s_{\alpha_{i+1}}, \dots\}$ we obtain $\{\dots, s_{\alpha_{i+1}}, s'_{\alpha_i}, \dots\}$. Performing a series of such elementary interchange operations, we can obtain any ordering starting from a given one.

The transformation in Fig. 4 is an example of the braid group transformation from Section 4.

After constructing a pattern with splitting of the fundamental domain into ideal triangles with vertices at the absolute (see Fig. 5), we can apply the above graph technique (cf. [12], [6]). We then have the spine with $|\delta|$ new pending edges pointed outward the fundamental domain and passing through the preimages of the \mathbb{Z}_2 -orbifold points. The corresponding Fuchsian group is then parameterized by real numbers Z_α associated to all the edges of the constructed graph.

We consider below the example of the Riemann surface with n \mathbb{Z}_2 -orbifold points and with one hole (puncture).

2.2 The group \mathfrak{G}_n

We consider the Poincaré disc with n different marked points s_i , $i = 1, \dots, n$ inside it. At each point s_i we introduce the element F_i of the rotation through π ; each $F_i = U_i F U_i^{-1}$ is a conjugate of the matrix (2.6).

We are interested in the group \mathfrak{G}_n generated by all the F_i . Observe, first, that the element $\gamma_{ij} = F_i F_j$ is always a hyperbolic element whose *invariant axis* is a unique geodesic that passes through the points s_i and s_j and its *length* is exactly the double geodesic distance between s_i and s_j . The fundamental domain necessarily has the form (an ideal polygon) depicted in Fig. 3; finite-length geodesic lines between the points s_i in Fig. 3 represent the above elements γ_{ij} .

We now set in the correspondence to the Poincaré disc with n orbifold points the tree fat graph with n pending edges. We present the result in Fig. 5.

2.3 Structure of geodesic lines and multicurves (laminations)

2.3.1 Geodesic functions corresponding to paths in graphs

To each closed path in a fat graph $\Gamma_{g,s,|\delta|}$, which is a spine of a genus g Riemann surface with s holes and $|\delta|$ \mathbb{Z}_2 -orbifold points, we set into a correspondence a closed path in the Riemann surface. This closed path is a closed geodesic being an image of the invariant axis of the corresponding hyperbolic element of the Fuchsian group. In the orbifold case, we have however a new class of finite-length geodesic paths. Namely, let us consider a path in the graph connecting two dot-vertices s_i and s_j (may be the same dot-vertex s_i) and going by exactly the same sequence of edges of the graph in the both directions (see

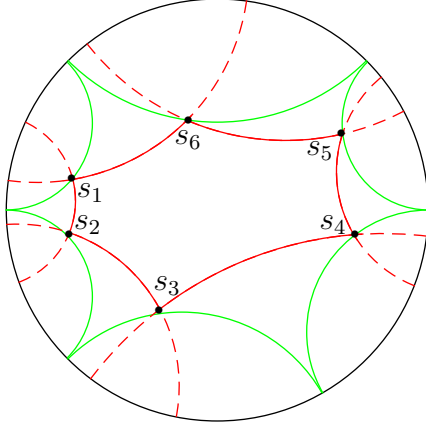


Figure 3: The Poincaré disc with $n = 6$ preimages s_i of orbifold points (marked by \bullet). These points lie on sides of an ideal polygon, and complementary geodesic lines in the figure are the invariant axes of elements $\gamma_{i,i+1} = F_i F_{i+1}$, the part of an axis that lies in the fundamental domain is drawn as the solid line and the outer part is drawn as a dashed line.

the example in Fig. 5). The corresponding element of the almost-hyperbolic Fuchsian group then has the form

$$A_{ij}^{-1} F_i A_{ij} F_j = \tilde{F}_i F_j \quad (2.8)$$

and, by the same reason as above, the invariant axis of this element passes exactly through the orbifold points s_i and s_j (and its length is again the doubled length of the corresponding path between these two points). The corresponding path in the orbifold Riemann surface has then s_i and s_j as its terminal points. We must therefore add to the set of smooth closed geodesic lines in the Riemann surface the set of all geodesic lines that start and terminate at the orbifold points (including cases where it is the same orbifold point).

Definition 3 The geodesic multicurve (GM), or lamination, for an orbifold Riemann surface $\Sigma_{g,s,|\delta|}$ is a set of non(self)intersecting geodesic lines (with multiplicities) including lines that terminate at the orbifold points. In the latter case, only one line (with the multiplicity) that terminates at a point s_i is allowed in a GM.

The algebraic counterpart of a GM is the *GM* function (we use the same notation as we believe it does not lead to a confusion)

$$GM := \prod_{\gamma \in GM} G_\gamma^{m_\gamma}, \quad (2.9)$$

where the product is over all geodesics γ entering the GM with the multiplicities m_γ .

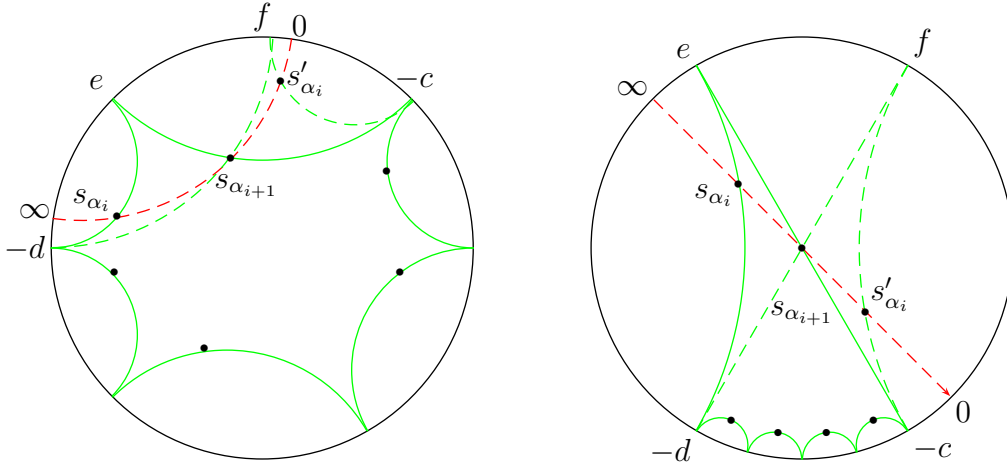


Figure 4: Changing the pattern of “natural” ordering when replacing the preimage s_{α_i} of an orbifold point by another preimage s'_{α_i} obtained upon rotation through the angle π about the neighbor preimage $s_{\alpha_{i+1}}$ of another orbifold point. Two bounding curves are replaced by two new bounding curves (dashed lines), the third dashed line is the geodesic line connecting s_{α_i} and $s_{\alpha_{i+1}}$ (and also s'_{α_i}). The equivalent form is presented in the right side where the point $s_{\alpha_{i+1}}$ is at the center of the disc; from the picture it is obvious that $\text{dist}(s_{\alpha_i}, s_{\alpha_{i+1}}) = \text{dist}(s_{\alpha_{i+1}}, s'_{\alpha_i})$.

3 Mapping class group transformations

3.1 Poisson structure

One of the most attractive properties of the graph description is a very simple Poisson algebra on the set of parameters Z_α . Namely, we have the following theorem. It was formulated for surfaces without marked points in [12] and was extended to *arbitrary graphs* with pending vertices in [14] (see also [3]).

Theorem 3.1 *In the coordinates Z_α on any fixed spine corresponding to a surface with orbifold points, the Weil–Petersson bracket B_{WP} is given by*

$$B_{WP} = \sum_v \sum_{i=1}^3 \frac{\partial}{\partial Z_{v_i}} \wedge \frac{\partial}{\partial Z_{v_{i+1}}}, \quad (3.1)$$

where the sum is taken over all three-valent (i.e., not pending) vertices v and v_i , $i = 1, 2, 3 \pmod 3$, are the labels of the cyclically ordered edges incident on this vertex irrespectively on whether they are internal or pending edges of the graph.

The center of this Poisson algebra is provided by the proposition.

Proposition 3.2 *The center of the Poisson algebra (3.1) is generated by elements of the form $\sum Z_\alpha$, where the sum ranges all edges of $\Gamma_{g,\delta}$ belonging to the same boundary component taken with multiplicities. This means, in particular, that each pending edge contributes twice to such sums. The dimension of this center is obviously s .*

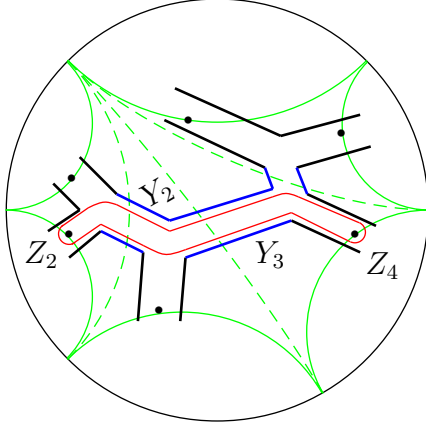


Figure 5: The Poincaré disc with $n = 6$ preimages \mathbb{Z}_2 -orbifold points s_i (marked by \bullet) with the associated fat graph that is dual to the ideal triangle decomposition of the fundamental domain (additional geodesics of ideal triangle partition inside the fundamental domain are drawn by dashed infinite lines). We associate real numbers Z_i , $i = 1, \dots, 6$, to the pending edges and real numbers Y_2 , Y_3 , and Y_4 to the inner edges (some of these parameters are indicated in the figure). The closed curve in the graph corresponds to $\text{tr } F_2 F_4$.

Example 3.1 Let us consider the graph in Fig. 6. It has two boundary components and two corresponding geodesic lines. Their lengths, $\sum_{i=1}^4 Y_i$ and $\sum_{i=1}^4 (Y_i + 2Z_i)$, are the two Casimirs of the Poisson algebra with the defining relations

$$\{Y_i, Y_{i-1}\} = 1 \pmod{4}, \quad \{Z_i, Y_i\} = -\{Z_i, Y_{i-1}\} = 1 \pmod{4},$$

and with all other brackets equal to zero.

3.2 Flip morphisms of fat graphs

In this section, we present the complete list of mapping class group transformations that enable us to change numbers $|\delta_k|$ of orbifold points associated with the k th hole, to change the cyclic ordering inside any of the sets δ_k , to flip any inner edge of the graph and, eventually, change the orientation of the geodesic spiraling to the hole perimeter (in the case where we have more than one hole).³ We can therefore establish a morphism between any two of the graphs belonging to the same class $\Gamma_{g,s,|\delta|}$.

3.2.1 Whitehead moves on inner edges

The Z_α -coordinates (which are the logarithms of cross ratios) are called (*Thurston*) *shear coordinates* [24],[1] in the case of punctured Riemann surface (without boundary components). We preserve this notation and this term also in the case of orbifold surfaces.

³On the language of cluster algebras [16, 14], this means that we are able to mutate *any* edge of any fat graph possibly with pending edges and, possibly, with inner edges starting and terminating at the same vertex.

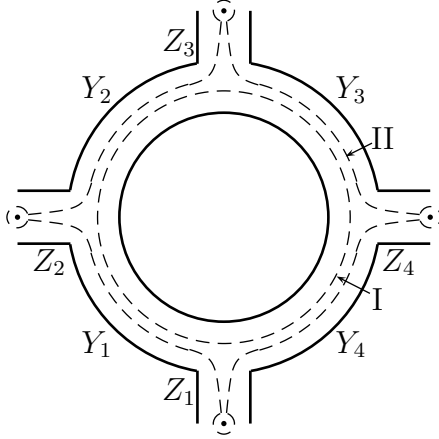


Figure 6: An example of geodesics whose geodesic functions G_I and G_{II} are in the center of the Poisson algebra (dashed lines).

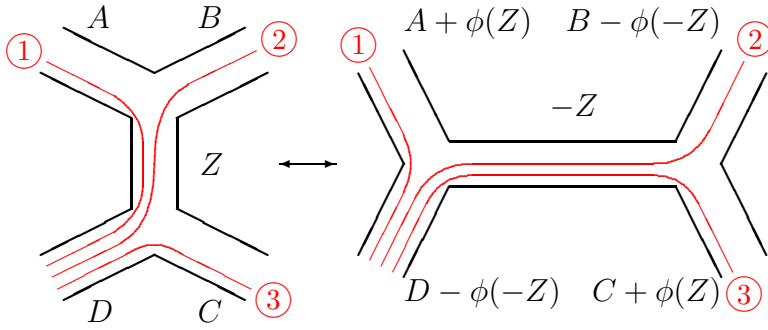


Figure 7: Flip, or Whitehead move on the shear coordinates Z_α . The outer edges can be pending, but the edge with respect to which the morphism is performed must be an internal edge.

In the case of surfaces with holes, Z_α are the coordinates on the Teichmüller space $\mathcal{T}_{g,s}^H$, which is the 2^s -fold covering of the standard Teichmüller space ramified over surfaces with punctures (when a hole perimeter becomes zero, see [13]). We set Z_α to be the coordinates of the corresponding spaces $\mathcal{T}_{g,|\delta_1|,|\delta_2|,\dots,|\delta_s|}^H$ in the orbifold case, where, as above, we let $|\delta_i|$ denote the number of orbifold points (may be zero) associated to the i th hole.

Given an enumeration of the edges of the spine Γ of Σ and assuming the edge α to have distinct endpoints, we may produce another spine Γ_α of Σ by contracting and expanding edge α of Γ , the edge labeled Z in Figure 7, to produce Γ_α as in the figure. Furthermore, an enumeration of the edges of Γ induces an enumeration of the edges of Γ_α in the natural way, where the vertical edge labelled Z in Figure 7 corresponds to the horizontal edge labelled $-Z$. We say that Γ_α arises from Γ by a *Whitehead move* (or flip) along the edge α . A labeling of edges of the spine Γ implies a natural labeling of edges of the spine Γ_α ; we then obtain a morphism between the spines Γ and Γ_α .

Proposition 3.3 [5] *Setting $\phi(Z) = \log(e^Z + 1)$ and adopting the notation of Fig. 7 for shear coordinates of nearby edges, the effect of a Whitehead move is as follows:*

$$W_Z : (A, B, C, D, Z) \rightarrow (A + \phi(Z), B - \phi(-Z), C + \phi(Z), D - \phi(-Z), -Z) \quad (3.2)$$

In the various cases where the edges are not distinct and identifying an edge with its shear coordinate in the obvious notation we have: if $A = C$, then $A' = A + 2\phi(Z)$; if $B = D$, then $B' = B - 2\phi(-Z)$; if $A = B$ (or $C = D$), then $A' = A + Z$ (or $C' = C + Z$); if $A = D$ (or $B = C$), then $A' = A + Z$ (or $B' = B + Z$). Any variety of edges among A , B , C , and D can be pending edges of the graph.

We also have two simple but important lemmas establishing the properties of invariance w.r.t. the flip morphisms [5].

Lemma 3.4 *Transformation (3.2) preserves the traces of products over paths (2.5).*

Lemma 3.5 *Transformation (3.2) preserves Poisson structure (3.1) on the shear coordinates.*

That the Poisson algebra for the orbifold Riemann surfaces case is invariant under the flip transformations follows immediately because we flip here inner, not pending, edges of a graph, which reduces the situation to the “old” statement for surfaces without orbifold points.

3.2.2 Whitehead moves on pending edges

In the case of orbifold surfaces we encounter a new phenomenon, namely, we can construct morphisms relating *any* two of the Teichmüller spaces $\mathcal{T}_{g,\delta^1}^H$ and $\mathcal{T}_{g,\delta^2}^H$ with $\delta^1 = \{|\delta_1^1|, \dots, |\delta_{s_1}^1|\}$ and $\delta^2 = \{|\delta_1^2|, \dots, |\delta_{s_2}^2|\}$ providing $s_1 = s_2 = s$ and $\sum_{i=1}^{s_1} |\delta_i^1| = \sum_{i=1}^{s_2} |\delta_i^2|$, that is, we explicitly construct morphisms relating any two of algebras corresponding to orbifold surfaces of the same genus, same number of boundary components, and with the same total number of orbifold points whose distributions into the holes can be arbitrary.

This new morphism corresponds in a sense to flipping a pending edge.

Lemma 3.6 *Transformation in Fig. 8 is the morphism between the spaces $\mathcal{T}_{g,\delta^1}^H$ and $\mathcal{T}_{g,\delta^2}^H$. These morphisms preserve both Poisson structures (3.1) and the geodesic functions. In Fig. 8 any (or both) of Y -variables can be variables of pending edges (the transformation formula is insensitive to it).*

In the ideal triangular decomposition of the original Riemann surface, this transformation reduces to changing the boundary geodesic line that starts at the corresponding orbifold point as shown in Fig. 9. There we assume Y_1 and Y_2 to be variables of internal edges. The two holes in the figure can be the same hole if the two boundary lines in Fig. 8 belong to the same boundary component.

Proof. Verifying the preservation of Poisson relations (3.1) is simple, whereas for traces over paths we have four cases, and in each of these cases we have the following 2×2 -matrix equalities (each can be verified directly)

$$\begin{aligned} X_{Y_2} L X_Z F X_Z L X_{Y_1} &= X_{\tilde{Y}_2} L X_{\tilde{Y}_1}, \\ X_{Y_1} R X_Z F X_Z R X_{Y_1} &= X_{\tilde{Y}_1} L X_{\tilde{Z}} F X_{\tilde{Z}} R X_{\tilde{Y}_1}, \\ X_{Y_2} R X_{Y_1} &= X_{\tilde{Y}_2} R X_{\tilde{Z}} F X_{\tilde{Z}} R X_{\tilde{Y}_1}, \\ X_{Y_2} L X_Z F X_Z R X_{Y_2} &= X_{\tilde{Y}_2} R X_{\tilde{Z}} F X_{\tilde{Z}} L X_{\tilde{Y}_2}, \end{aligned}$$

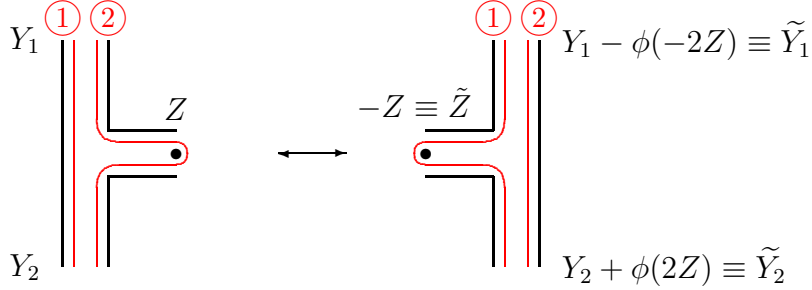


Figure 8: Flip, or Whitehead move on the shear coordinates when flipping the pending edge Z (indicated by bullet). Any (or both) of edges Y_1 and Y_2 can be pending.

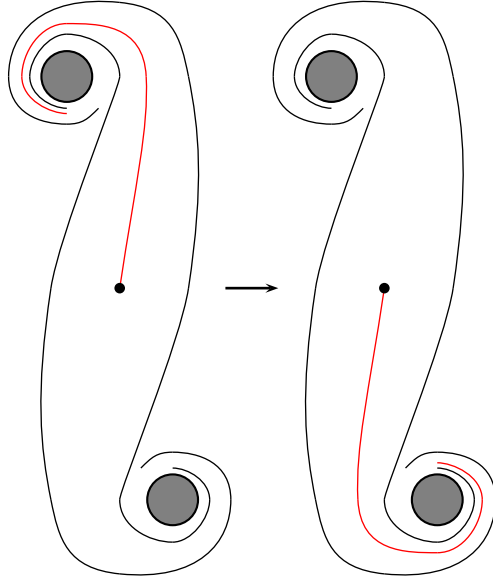


Figure 9: Changing ideal triangular decomposition corresponding to transformation in Fig. 8.

where (in the exponentiated form)

$$e^{\tilde{Y}_1} = e^{Y_1}(1 + e^{-2Z})^{-1}, \quad e^{\tilde{Y}_2} = e^{Y_2}(1 + e^{2Z}), \quad e^{\tilde{Z}} = e^{-Z}. \quad \square \quad (3.3)$$

From the technical standpoint, all these equalities follow from flip transformation (3.2) upon the substitution $A = C = Y_2$, $B = D = Y_1$, and $Z = 2Z$. The above four cases of geodesic functions are then exactly four possible cases of geodesic arrangement in the (omitted) proof of Lemma 3.4.

Using flip morphisms in Fig. 8 and in formula (3.2), we establish a morphism between any two algebras corresponding to surfaces of the same genus, same number of boundary components, and same total number of marked points on these components. And it is again a standard tool that if, after a series of morphisms, we come to a graph of the same combinatorial type as the initial one (disregarding labeling of edges), we associate a *mapping class group* operation to this morphism therefore passing from the groupoid of morphisms to the group of modular transformations.

Example 3.2 The flip morphism w.r.t. the edge Z_1 in the pattern in (3.4),

$$(3.4)$$

where Z_1 and Z_2 are the pending edges, generates the (unitary) mapping class group transformation

$$e^{Z_2} \rightarrow e^{-Z_1}, \quad e^{Z_1} \rightarrow e^{Z_2}(1 + e^{-2Z_1})^{-1}, \quad e^Y \rightarrow e^Y(1 + e^{2Z_1}) \quad (3.5)$$

on the corresponding Teichmüller space $\mathcal{T}_{g,\delta}^H$. This is one of the generators of the *braid group* [3].

3.2.3 Changing the spiraling direction

We introduce a new mapping class group transformation that change the sign of the hole perimeter:

$$(3.6)$$

That this transformation preserves geodesic functions follows from two matrix equalities:

$$\begin{aligned} X_Y L X_X L X_Y &= X_{Y+X} L X_{-X} L X_{Y+X}, \\ X_Y R X_X R X_Y &= X_{Y+X} R X_{-X} R X_{Y+X}, \end{aligned}$$

and we can correspondingly enlarge the mapping class group of $\mathcal{T}_{g,\delta}^H$ by adding symmetries between sheets of the 2^s -ramified covering of the “genuine” (nondecorated) Teichmüller space $\mathcal{T}_{g,\delta}$.

The geometrical meaning of this transformation is clear: we change the direction of spiraling to the hole perimeter line for all lines of the ideal triangle decomposition that spiral to a given hole.

3.3 The graphical representation

In the case of usual geodesic functions, there exists a very convenient representation in which one can apply classical skein and Poisson relations in classical case or the quantum skein relation in the quantum case and ensure the Reidemeister moves when “disentangling” the products of geodesic function representing them as linear combinations of multicurve functions. However, in our case, it is still obscure what happens when geodesic lines intersect in some way at the dot vertex. In fact, we can propose the comprehensive

graphical representation in this case as well! For this, we turn to Fig. 1 and assume that the inversion matrix F corresponds to actual winding around this dot-vertex as shown in the figure.

We now formulate the rules for geodesic algebra that follow from relations (3.1) and classical skein relations. They coincide with the rules in the case of surfaces with holes except the one new nontrivial case depicted in Fig. 10. Note that all claims below follow from direct and explicit calculations involving representations from Sec. 2.

3.3.1 Classical skein relation

The trace relation $\text{tr}(AB) + \text{tr}(AB^{-1}) - \text{tr} A \cdot \text{tr} B = 0$ for arbitrary 2×2 matrices A and B with unit determinant allows one to “disentangle” any product of geodesic functions $G_A \cdot G_B$, i.e., express it uniquely as a finite linear combination of generalized multicurves (see Definition 3). This relation corresponds to resolving the crossing between two geodesics A and B as indicated in the formula below and it is referred to as the *skein relation*.

$$(3.7)$$

3.3.2 Poisson brackets for geodesic functions.

We first mention that two geodesic functions Poisson commute if the underlying geodesics are disjointly embedded in the sense of the new graph technique involving dot-vertices. Because of the Leibnitz rule for the Poisson bracket, it suffices to consider only “simple” intersections of pairs of geodesics when the respective geodesic functions G_1 and G_2 are

$$G_1 = \text{tr} \dots X_C R X_Z L X_A \dots, \quad (3.8)$$

$$G_2 = \text{tr} \dots X_B L X_Z R X_D \dots. \quad (3.9)$$

The positions of edges A, B, C, D , and Z are as in Fig. 7. Ellipses in (3.8), (3.9) refer to arbitrary sequences of matrices R, L, X_{Z_i} , and F ; G_1 and G_2 must correspond to closed geodesic lines, but are otherwise arbitrary.

Direct calculations then give

$$\{G_1, G_2\} = \frac{1}{2}(G_{AB^{-1}} - G_{AB}), \quad (3.10)$$

in the notation of (3.7) where we set $G_1 = G_A$ and $G_2 = G_B$. Then $G_{AB^{-1}}$ corresponds to the geodesic that passes over the edge Z twice, so it has the form $\text{tr} \dots X_C R_Z R_D \dots \dots X_B L_Z L_A \dots$. These relations were first obtained by Goldman [17] in the continuous parametrization (the classical Turaev–Viro algebra).

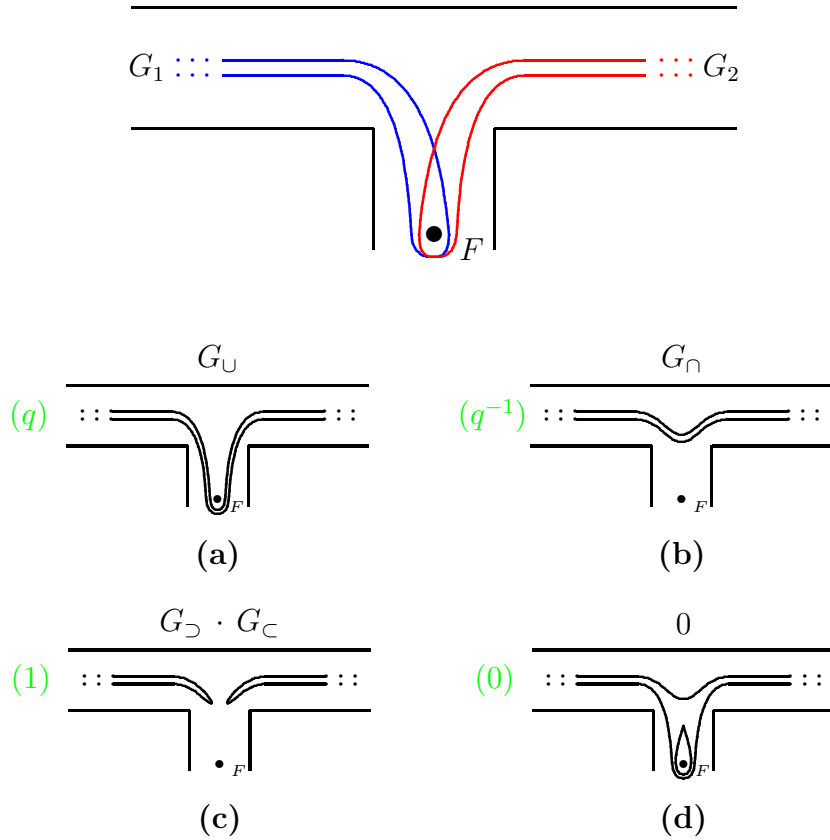


Figure 10: An example of two geodesic lines intersecting at the dot-vertex. We present four homotopical types of resolving two intersections in this pattern (Cases (a)–(d)). A multicurve in Case (d) contains the loop with only the dot-vertex inside. This loop is $\text{tr } F = 0$, so the whole contribution vanishes in this case. The factors in brackets pertain to the quantum case in Sec. 5 indicating the weights with which the corresponding (quantum) geodesic multicurves enter the expression for the quantum operatorial product $G_1^{\hbar} G_2^{\hbar}$.

Given two curves, γ_1 and γ_2 , with an arbitrary number of crossings, we now find their Poisson bracket using the following rules:

- We take a sum of products of geodesic functions of non(self)intersecting curves obtained when we apply Poisson relation (3.10) at one intersection point and classical skein relation (3.7) at all the remaining points of intersection; we assume the summation over all possible cases.
- If, in the course of calculation, we meet an empty (contractible) loop, then we associate the factor -2 to such a loop; this assignment, as is known [8], ensures the Reidemeister moves on the set of geodesic lines thus making the bracket to depend only on the homotopical class of the curve embedding in the surface.
- If, in the course of calculation, we meet a curve homeomorphic to passing around a dot-vertex, then we set $\text{tr } F = 0$ thus killing the whole corresponding multicurve function.

All these rules are equivalently applicable to the intersections of the geodesic lines depicted in Fig. 10; the result is presented in the figure. In obvious notation, $\{G_1, G_2\} = G_{\cup} - G_{\cap}$.

Because the Poisson relations are completely determined by homotopy types of curves, using Lemma 3.6, we immediately come to the theorem below.

Theorem 3.7 *Poisson algebras of geodesic functions for two orbifold Riemann surfaces $\Sigma_{g,s,\{\delta_1,\dots,\delta_s\}}$ and $\Sigma_{g,s,\{\tilde{\delta}_1,\dots,\tilde{\delta}_s\}}$ with $\sum_{k=1}^s |\delta_k| = \sum_{k=1}^s |\tilde{\delta}_k|$ are isomorphic; the isomorphism is described by Lemma 3.6.*

In particular, it follows from this theorem that we can always collect all the marked points on just one boundary component.

4 Poisson and braid-group relations for A_n and D_n

4.1 Special algebras of geodesic functions

We now demonstrate two cases where it is possible to close the Poisson geodesic algebras on the level of finite number of elements.⁴ In all examples below, we can attain such a closure for a price of introducing nonlinear terms in the right-hand sides of Poisson relations.

4.1.1 The A_n algebras

Consider the disc with n orbifold points; examples of the corresponding representing graph Γ_n are depicted in Fig. 11 for $n = 3, 4, \dots$. We enumerate the n dot-vertices clockwise, $i, j = 1, \dots, n$. We then let G_{ij} with $i < j$ denote the geodesic function corresponding to the geodesic line that encircles exactly two dot-vertices with the indices i and j . The corresponding geodesic line is the line connecting the preimages s_i and s_j in Fig. 3 and the distance is double the geodesic distance between these points. Three algebraic functions, G_{12} , G_{23} , and G_{13} , correspond to the lines in Fig. 11.

Using the skein relation, we can close the Poisson algebra thus obtaining for A_3 :

$$\{G_{12}, G_{23}\} = G_{12}G_{23} - 2G_{13} \text{ and cycl. permut.} \quad (4.1)$$

In higher-order algebras (starting with $n = 4$), we meet a more complicate case of the fourth-order crossing (as shown in the case $n = 4$ in Fig. 11). The corresponding Poisson brackets are

$$\{G_{13}, G_{24}\} = 2G_{12}G_{34} - 2G_{14}G_{23} \quad (4.2)$$

(note that the r.h.s. is a linear combination of multicurves).

Algebraic relations (4.1) and (4.2) are exactly the Nelson–Regge [21] relations in algebras of geodesics on Riemann surfaces with one and two holes [6], and we can use the well-developed machinery for dealing with these algebras. These algebras also appear in the Frobenius manifold approach [9].

⁴Besides these two cases among which the case of A_n algebra is equivalent to the Nelson–Regge algebra, the only other case where it is possible is the case of sphere with four holes.

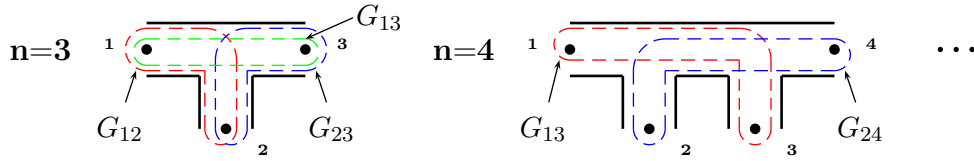


Figure 11: Generating graphs for A_n algebras for $n = 3, 4, \dots$. We indicate character geodesics whose geodesic functions G_{ij} enter bases of the corresponding algebras.

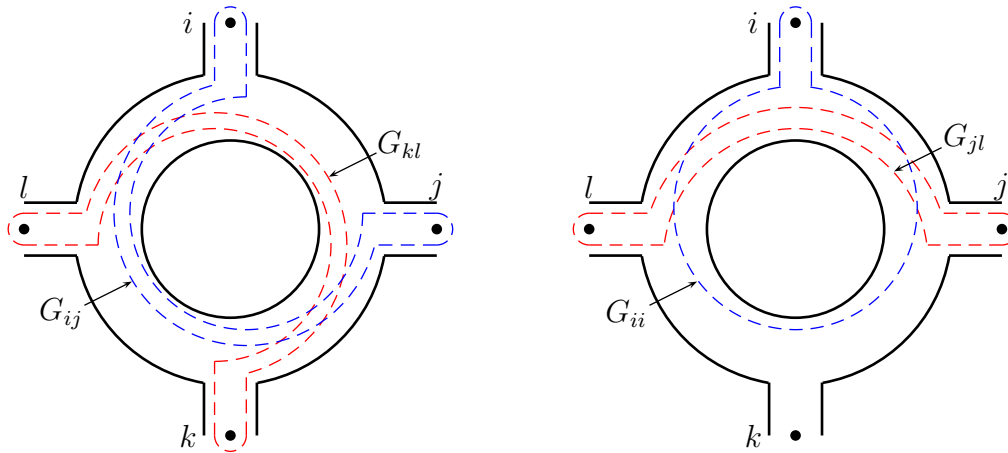


Figure 12: Typical geodesics corresponding to the geodesic functions constituting a set of generators of the D_n algebra. We let G_{ij} , $i, j = 1, \dots, n$, denote these functions. The order of subscripts indicates the direction of encompassing the hole (the second boundary component of the annulus). The most involved pattern of intersection is on the left part of the figure: the geodesics have there eight-fold intersection; in the right part we present also the geodesic function G_{ii} corresponding to the geodesic that encircles exactly one orbifold point and the central hole.

4.1.2 The D_n -algebras

We now consider the case of annulus with n orbifold points associated to one of the boundary component (see the example in Fig. 6. In this case, a finite set of geodesic functions closed w.r.t. the Poisson brackets is given by geodesic functions corresponding to geodesics in Fig. 12

We therefore describe a set of geodesic functions by the matrix G_{ij} with $i, j = 1, \dots, n$ where the order of indices indicates the direction of encompassing the second boundary component of the annulus. The corresponding geodesics for $i \neq j$ connect pairwise the points s_i and s_j encompassing the “central” hole from one or another side. Counterintuitively, the geodesic function G_{ii} does not correspond to the geodesic line that starts and terminates at the point s_i encompassing the hole; instead we must take a smooth (closed) geodesic line that encircles the hole and the given orbifold point.

Lemma 4.1 *The set of geodesic functions G_{ij} corresponding to geodesics in Fig. 12 is Poisson closed.*

We present below all the nontrivial Poisson relations in the graphical way; because

of the rotational symmetry, only the cyclic order w.r.t. the central hole matters; the starting vertex (with the number one) can be any among the dot-vertices around the hole; the Roman numbers I and II indicate which geodesic function occupies the first and which—the second place in the corresponding Poisson bracket.

We have six basic nontrivial brackets (ordered by increasing complexity)

a.

$$2 \left(\text{Figure-eight with loops I and II} \right) = -2 \left(\text{Two vertical loops} \right) - 2 \left(\text{Figure-eight with loops} \right)$$

(4.3)

reduction **a₁**

$$\left(\text{Figure-eight with loops I and II} \right) = \left(\text{Figure-eight with loops I and II} \right) - 2 \left(\text{Figure-eight with loop} \right)$$

(4.4)

b.

$$2 \left(\text{Figure-eight with loops I and II} \right) = -2 \left(\text{Two diagonal loops} \right) - 2 \left(\text{Figure-eight with diagonal loops} \right)$$

(4.5)

reduction **b₁**

$$\left(\text{Figure-eight with loops I and II} \right) = \left(\text{Figure-eight with loops I and II} \right) - 2 \left(\text{Figure-eight with diagonal loop} \right)$$

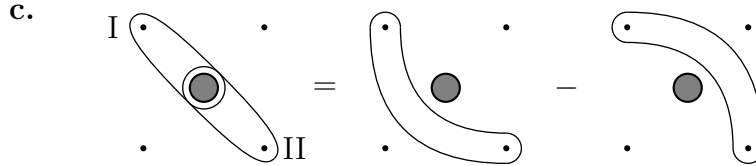
(4.6)

reduction **b₂**

$$\left(\text{Figure-eight with loops I and II} \right) = - \left(\text{Figure-eight with loops I and II} \right) + 2 \left(\text{Figure-eight with diagonal loop} \right)$$

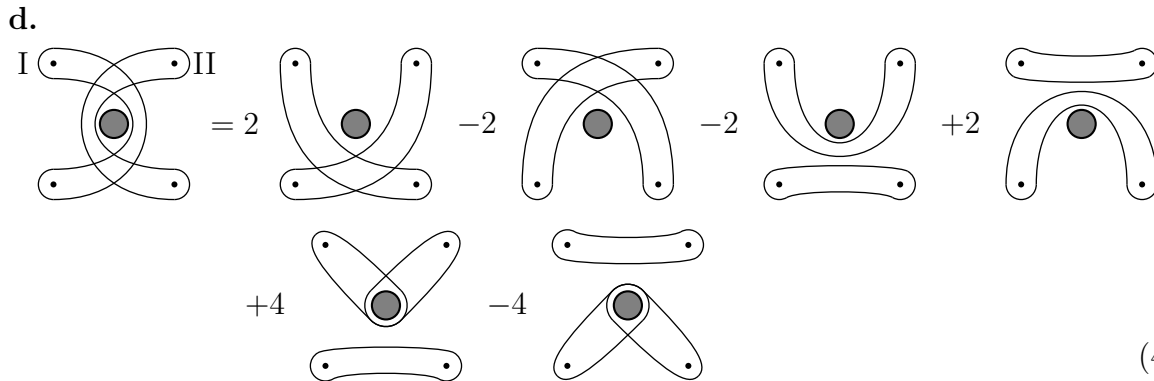
(4.7)

c.



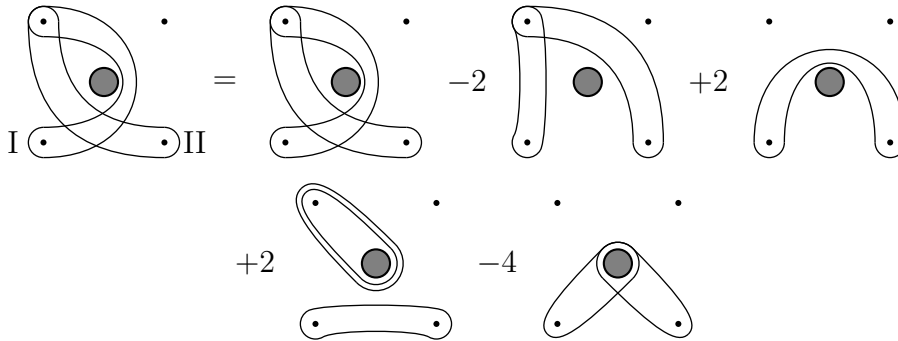
$$(4.8)$$

d.



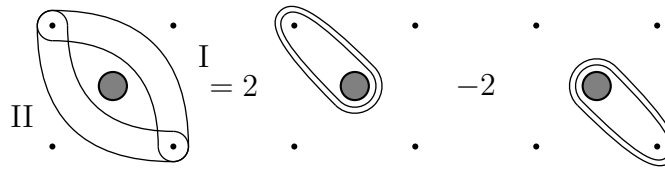
$$(4.9)$$

reduction \mathbf{d}_1



$$(4.10)$$

reduction \mathbf{d}_2



$$(4.11)$$

4.2 Braid group relations for geodesic algebras

The mapping class group transformation that is a generator of a braid group was presented in Example 3.2 and pertains to interchanging two neighbor orbifold points. It turns out that such transformations generate the whole mapping class group in the case of A_n and D_n algebras (in the latter case, we must also add the transformation interchanging the n th and the first orbifold points as an independent generator).

Then, the action of the braid group generator $R_{i,i+1}$ on \mathcal{A} can be presented in the form of usual matrix product:

$$R_{i,i+1}\mathcal{A} = B_{i,i+1}\mathcal{A}B_{i,i+1}^T \quad (4.16)$$

with $B_{i,i+1}^T$ the matrix transposed to $B_{i,i+1}$.

We now consider the action of the chain of transformations $R_{n-1,n}R_{n-2,n-1}\dots R_{2,3}R_{1,2}\mathcal{A}$. Note that, on each step, the item $G_{i,i+1}^{(i-1)}$ in the corresponding matrix $B_{i,i+1}$ is the transformed quantity (we assume $G_{ij}^{(0)}$ to coincide with the initial G_{ij} in \mathcal{A}). However, it is easy to see that for just this chain of transformations, $G_{i,i+1}^{(i-1)} = G_{1,i+1}^{(0)} = G_{1,i+1}$, and the whole chain of matrices B can be then expressed in terms of the initial variables $G_{i,j}$ as

$$\mathcal{B} \equiv B_{n-1,n}B_{n-2,n-1}\dots B_{2,3}B_{1,2} = \begin{pmatrix} G_{1,2} & -1 & 0 & \dots & 0 \\ G_{1,3} & 0 & -1 & & \vdots \\ \vdots & \vdots & \ddots & \ddots & 0 \\ G_{1,n} & 0 & \dots & 0 & -1 \\ 1 & 0 & \dots & 0 & 0 \end{pmatrix}, \quad (4.17)$$

whereas its action on \mathcal{A} gives

$$\tilde{\mathcal{A}} \equiv \mathcal{B}\mathcal{A}\mathcal{B}^T = \begin{pmatrix} 1 & G_{2,3} & G_{2,4} & \dots & G_{2,n} & G_{1,2} \\ 0 & 1 & G_{3,4} & \dots & G_{3,n} & G_{1,3} \\ 0 & 0 & 1 & & G_{4,n} & G_{1,4} \\ \vdots & \vdots & & \ddots & & \vdots \\ 0 & 0 & \dots & 0 & 1 & G_{1,n} \\ 0 & 0 & \dots & \dots & 0 & 1 \end{pmatrix}, \quad (4.18)$$

which is a mere permutation of the elements of the initial matrix \mathcal{A} . It is easy to see that the n th power of this permutation gives the identical transformation, so we obtain the last *braid group relation*.

Lemma 4.3 *For any $n \geq 3$, we have the second braid group relation for the A_n algebra:*

$$(R_{n-1,n}R_{n-2,n-1}\dots R_{2,3}R_{1,2})^n = Id. \quad (4.19)$$

4.2.2 Central elements of Poisson/braid group transformations for A_n algebras

From (4.16), we immediately obtain that the same braid-group transformation holds for the transposed matrix \mathcal{A}^T and therefore for any combination $\lambda\mathcal{A} + \lambda^{-1}\mathcal{A}^T$:

$$R_{i,i+1}(\lambda\mathcal{A} + \lambda^{-1}\mathcal{A}^T) = B_{i,i+1}(\lambda\mathcal{A} + \lambda^{-1}\mathcal{A}^T)B_{i,i+1}^T, \quad (4.20)$$

and the determinant

$$\det(\lambda\mathcal{A} + \lambda^{-1}\mathcal{A}^T) \quad (4.21)$$

is therefore the generating function for the central elements of the Poisson algebra and, simultaneously, the invariants of the braid group in the A_n case. There are $\lfloor \frac{n}{2} \rfloor$ such independent elements (due to the symmetry $\lambda \leftrightarrow \lambda^{-1}$, so the maximum Poisson dimension of the corresponding A_n algebra is $\frac{n(n-1)}{2} - \lfloor \frac{n}{2} \rfloor$ (an even number for all n)).

4.2.3 Braid group relations for geodesic functions of D_n -algebras

It is possible to express readily the action of the braid group on the level of the geodesic functions $G_{i,j}$, $i, j = 1, \dots, n$, interpreted also as entries of the $n \times n$ -matrix \mathcal{D} (the elements that are not indicated remain invariant):

$$R_{i,i+1}\mathcal{D} = \tilde{\mathcal{D}}, \text{ where } \begin{cases} \tilde{G}_{i+1,k} = G_{i,k} & k \neq i, i+1, \\ \tilde{G}_{i,k} = G_{i,k}G_{i,i+1} - G_{i+1,k} & k \neq i, i+1, \\ \tilde{G}_{k,i+1} = G_{k,i} & k \neq i, i+1, \\ \tilde{G}_{k,i} = G_{k,i}G_{i,i+1} - G_{k,i+1} & k \neq i, i+1, \\ \tilde{G}_{i,i+1} = G_{i,i+1} \\ \tilde{G}_{i+1,i+1} = G_{i,i} \\ \tilde{G}_{i,i} = G_{i,i}G_{i,i+1} - G_{i+1,i+1} \\ \tilde{G}_{i+1,i} = G_{i+1,i} + G_{i,i+1}G_{i,i}^2 - 2G_{i,i}G_{i+1,i+1} \end{cases} . \quad (4.22)$$

To obtain the full mapping class group, we must complete this set of transformations by the new element $R_{n,1}$ interchanging s_1 and s_n :

$$R_{n,1}\mathcal{D} = \tilde{\mathcal{D}}, \text{ where } \begin{cases} \tilde{G}_{1,k} = G_{n,k} & k \neq n, 1, \\ \tilde{G}_{n,k} = G_{n,k}G_{n,1} - G_{1,k} & k \neq n, 1, \\ \tilde{G}_{k,1} = G_{k,n} & k \neq n, 1, \\ \tilde{G}_{k,n} = G_{k,n}G_{n,1} - G_{k,1} & k \neq n, 1, \\ \tilde{G}_{n,1} = G_{n,1} \\ \tilde{G}_{1,1} = G_{n,n} \\ \tilde{G}_{n,n} = G_{n,n}G_{n,1} - G_{1,1} \\ \tilde{G}_{1,n} = G_{1,n} + G_{n,1}G_{n,n}^2 - 2G_{n,n}G_{1,1} \end{cases} . \quad (4.23)$$

The first braid group relation follows in this case as well from the three-step process, but it can be also verified explicitly that the following lemma holds just on the level of elements $G_{i,j}$.

Lemma 4.4 *For any $n \geq 3$, we have the braid group relation for transformations (4.22), (4.23):*

$$R_{i-1,i}R_{i,i+1}R_{i-1,i}\mathcal{D} = R_{i,i+1}R_{i-1,i}R_{i,i+1}\mathcal{D}, i = 1, \dots, n \text{ mod } n. \quad (4.24)$$

Note that the second braid-group relation (see Lemma 4.3) is lost in the case of D_n -algebras.

Presenting the braid-group action in the matrix-action (covariant) form (4.16) turned out to be a nontrivial problem. First, it was noted already in [3] that special combinations of G_{ij} admit similar transformation laws under the subgroup of braid-group transformations generated by relations (4.22) alone (omitting the last transformation (4.23)).

Consider two new $n \times n$ matrices composed from G_{ij} :

$$(\mathcal{R})_{i,j} = \begin{cases} -G_{j,i} - G_{i,j} + G_{i,i}G_{j,j} & j > i \\ G_{j,i} + G_{i,j} - G_{i,i}G_{j,j} & j < i \\ 0 & j = i \end{cases}, \quad (4.25)$$

$$(\mathcal{S})_{i,j} = G_{i,i}G_{j,j} \quad \text{for all } 1 \leq i, j \leq n; \quad (4.26)$$

here \mathcal{R} is skewsymmetric ($\mathcal{R}^T = -\mathcal{R}$) and \mathcal{S} is symmetric ($\mathcal{S}^T = \mathcal{S}$). Then, together with \mathcal{A} given by the old formula (4.12), we have the following statement.

Lemma 4.5 *Any linear combination $w_1\mathcal{A} + w_2\mathcal{A}^T + \rho\mathcal{R} + \sigma\mathcal{S}$ with complex $w_1, w_2, \rho,$ and σ transforms by formula (4.16) under the subgroup (4.22) of the braid group.*

However, incorporating the last generator of the braid group took a long time. Here, we present the new result obtained recently in collaboration with M. Mazzocco [7]⁵

Let us introduce the $(4n) \times (4n)$ upper triangular block matrix \mathbb{A} :

$$\mathbb{A} = \begin{bmatrix} \mathcal{A} & B & C & B^T \\ 0 & \mathcal{A} & B & C \\ 0 & 0 & \mathcal{A} & B \\ 0 & 0 & 0 & \mathcal{A} \end{bmatrix}, \quad \text{where } \begin{cases} B = \mathcal{S} + \mathcal{R} + \mathcal{A} - \mathcal{A}^T, \\ C = 2\mathcal{S} - \mathcal{A} - \mathcal{A}^T, C^T = C. \end{cases} \quad (4.27)$$

The matrices of braid-group transformations $R_{i,i+1}$ with $i = 1, \dots, n-1$, $\mathbb{B}_{i,i+1}$, have a simple block-diagonal structure:

$$\mathbb{B}_{i,i+1} = \begin{bmatrix} B_{i,i+1} & 0 & 0 & 0 \\ 0 & B_{i,i+1} & 0 & 0 \\ 0 & 0 & B_{i,i+1} & 0 \\ 0 & 0 & 0 & B_{i,i+1} \end{bmatrix}, \quad (4.28)$$

whereas a new matrix $\mathcal{B}_{n,1}(\lambda)$ must depend on the parameter λ and has the form

⁵The way to come to this result is interesting by itself; it involves some new insight on the whole topic. Here we, however, confine ourselves to a mere presentation, the reader can find details in [7].

$$\mathbb{B}_{n,1}(\lambda) = \left(\begin{array}{c|c|c|c} 0 & & & \lambda^2 \\ & \mathcal{I} & & \\ & & G_{1,n} & -1 \\ \hline & 1 & 0 & \\ & & \mathcal{I} & \\ & & & G_{1,n} & -1 \\ \hline & & 1 & 0 & \\ & & & \mathcal{I} & \\ & & & & G_{1,n} & -1 \\ \hline & & & 1 & 0 & \\ & & & & \mathcal{I} & \\ -\lambda^{-2} & & & & & G_{1,n} \end{array} \right), \quad (4.29)$$

with \mathcal{I} being the $(n-2) \times (n-2)$ unit matrices on the diagonal.

We then have the theorem.

Theorem 4.6 *The braid group relations (4.22) and (4.23) can be presented in the form of matrix relations for the matrix $\lambda\mathbb{A} + \lambda^{-1}\mathbb{A}^T$ with the matrix \mathbb{A} defined in (4.27):*

$$R_{i,i+1}(\lambda\mathbb{A} + \lambda^{-1}\mathbb{A}^T) = \mathbb{B}_{i,i+1}(\lambda\mathbb{A} + \lambda^{-1}\mathbb{A}^T)\mathbb{B}_{i,i+1}^T, \quad i = 1, \dots, n-1 \quad (4.30)$$

$$R_{n,1}(\lambda\mathbb{A} + \lambda^{-1}\mathbb{A}^T) = \mathbb{B}_{n,1}(\lambda)(\lambda\mathbb{A} + \lambda^{-1}\mathbb{A}^T)\mathbb{B}_{n,1}^T(\lambda^{-1}), \quad (4.31)$$

with $\mathbb{B}_{i,i+1}$ from (4.28) and $\mathbb{B}_{n,1}(\lambda)$ from (4.29).

4.2.4 Central elements of Poisson/braid group transformations for D_n algebras

Proceeding with analogy from the case of the A_n algebra, we take the determinant

$$\det(\lambda\mathbb{A} + \lambda^{-1}\mathbb{A}^T) \quad (4.32)$$

as the generating function for the central elements of the D_n algebra. This is a $(4n) \times (4n)$ -matrix, so one could expect the existence of $\left[\frac{4n}{2}\right] = 2n$ central elements. However, this matrix has a special structure, and if we take it for $\lambda = 1$, that is, consider the symmetric matrix $\mathbb{A} + \mathbb{A}^T$ (of a bilinear form), then, in terms of original matrices \mathcal{A} , \mathcal{S} , and \mathcal{R} , we have for $\mathbb{A} + \mathbb{A}^T$ the expression

$$\left[\begin{array}{c|c|c|c} \mathcal{A} + \mathcal{A}^T & \mathcal{S} + \mathcal{R} + \mathcal{A} - \mathcal{A}^T & 2\mathcal{S} - \mathcal{A} - \mathcal{A}^T & \mathcal{S} - \mathcal{R} - \mathcal{A} + \mathcal{A}^T \\ \hline \mathcal{S} - \mathcal{R} - \mathcal{A} + \mathcal{A}^T & \mathcal{A} + \mathcal{A}^T & \mathcal{S} + \mathcal{R} + \mathcal{A} - \mathcal{A}^T & 2\mathcal{S} - \mathcal{A} - \mathcal{A}^T \\ \hline 2\mathcal{S} - \mathcal{A} - \mathcal{A}^T & \mathcal{S} - \mathcal{R} - \mathcal{A} + \mathcal{A}^T & \mathcal{A} + \mathcal{A}^T & \mathcal{S} + \mathcal{R} + \mathcal{A} - \mathcal{A}^T \\ \hline \mathcal{S} + \mathcal{R} + \mathcal{A} - \mathcal{A}^T & 2\mathcal{S} - \mathcal{A} - \mathcal{A}^T & \mathcal{S} - \mathcal{R} - \mathcal{A} + \mathcal{A}^T & \mathcal{A} + \mathcal{A}^T \end{array} \right], \quad (4.33)$$

and adding first line of blocks to the third line and second to the fourth, we obtain the matrix in which two last lines of blocks are composed from the same matrix $2\mathcal{S}$. By its structure, the matrix \mathcal{S} has rank one being the outer product of two vectors, so we conclude that the matrix $\mathbb{A} + \mathbb{A}^T$ has at most rank $2n + 1$, that is, taking into account the symmetry $\lambda \leftrightarrow \lambda^{-1}$, we have

$$\det(\lambda\mathbb{A} + \lambda^{-1}\mathbb{A}^T) = (\lambda - \lambda^{-1})^{2n-1} \left[\lambda^{2n+1} + S_1\lambda^{2n-1} + \dots \right. \\ \left. \dots + S_n\lambda - S_n\lambda^{-1} - \dots - S_1\lambda^{1-2n} - \lambda^{-2n-1} \right], \quad (4.34)$$

so, in total, we have exactly n independent central elements S_i , $i = 1, \dots, n$, and the highest Poisson leaf dimension is $n^2 - n = n(n - 1)$.

5 Quantum Teichmüller spaces of orbifold Riemann surfaces

5.1 Canonical quantization of the Poisson algebra

A quantization of a Poisson manifold, which is equivariant under the action of a discrete group \mathcal{D} , is a family of $*$ -algebras \mathcal{A}^{\hbar} depending on a positive real parameter \hbar with \mathcal{D} acting by outer automorphisms and having the following properties:

1. (Flatness.) All algebras are isomorphic (noncanonically) as linear spaces.
2. (Correspondence.) For $\hbar = 0$, the algebra is isomorphic as a \mathcal{D} -module to the $*$ -algebra of complex-valued functions \mathcal{A}^0 on the Poisson manifold.
3. (Classical Limit.) The Poisson bracket on \mathcal{A}^0 given by $\{a_1, a_2\} = \lim_{\hbar \rightarrow 0} \frac{[a_1, a_2]}{\hbar}$ coincides with the Poisson bracket given by the Poisson structure of the manifold.

Fix a three-valent fatgraph $\Gamma_{g,\delta}$ as a spine of $\Sigma_{g,\delta}$, and let $\mathcal{T}^{\hbar} = \mathcal{T}^{\hbar}(\Gamma_{g,\delta})$ be the algebra generated by the operators Z_{α}^{\hbar} , one generator for each unoriented edge α of $\Gamma_{g,\delta}$, with relations

$$[Z_{\alpha}^{\hbar}, Z_{\beta}^{\hbar}] = 2\pi i \hbar \{Z_{\alpha}, Z_{\beta}\} \quad (5.1)$$

(cf. (3.1)) and the $*$ -structure

$$(Z_{\alpha}^{\hbar})^* = Z_{\alpha}^{\hbar}, \quad (5.2)$$

where Z_{α} and $\{\cdot, \cdot\}$ denotes the respective coordinate functions and the Poisson bracket on the classical Teichmüller space. Because of (3.1), the right-hand side of (5.1) is a constant taking only five values 0 , $\pm 2\pi i \hbar$, and $\pm 4\pi i \hbar$ depending upon five variants of identifications of endpoints of edges labelled α and β .

All the standard statements that we have in the case of Teichmüller spaces of Riemann surfaces with holes are transferred to the case of orbifold Riemann surfaces.

Lemma 5.1 *The center \mathcal{Z}^{\hbar} of the algebra \mathcal{T}^{\hbar} is generated by the sums $\sum_{\alpha \in I} Z_{\alpha}^{\hbar}$ over all edges $\alpha \in I$ surrounding a given boundary component, the center has dimension s , and the quantum structure is nondegenerate on the quotient $\mathcal{T}^{\hbar}/\mathcal{Z}^{\hbar}$.*

The examples of the *boundary-parallel* curves whose quantum lengths are the Casimir operators are again in Fig. 6. Of course, those are the same curves that provide the center of the Poisson algebra.

Corollary 5.2 *There is a basis for $\mathcal{T}^{\hbar}/\mathcal{Z}^{\hbar}$ given by operators p_i, q_i , for $i = 1, \dots, 3g - 3 + s + \sum_{j=1}^s |\delta_j|$ satisfying the standard commutation relations $[p_i, q_j] = 2\pi i \hbar \delta_{ij}$.*

5.2 Quantum flip transformations

The Whitehead move becomes now a morphism of (quantum) algebras. The *quantum Whitehead moves* or quantum *flips* along an edge Z of Γ are now described by Eq. (3.2), Fig. 8, and Eq. 3.4 with the (quantum) function [11], [5]

$$\phi(z) \equiv \phi^{\hbar}(z) = -\frac{\pi \hbar}{2} \int_{\Omega} \frac{e^{-ipz}}{\sinh(\pi p) \sinh(\pi \hbar p)} dp, \quad (5.3)$$

where the contour Ω goes along the real axis bypassing the origin from above. For each unbounded self-adjoint operator Z^{\hbar} on the Hilbert space \mathcal{H} of L^2 -functions, $\phi^{\hbar}(Z^{\hbar})$ is a well-defined unbounded self-adjoint operator on \mathcal{H} .

The function $\phi^{\hbar}(Z)$ satisfies the relations (see [5])

$$\begin{aligned} \phi^{\hbar}(Z) - \phi^{\hbar}(-Z) &= Z, \\ \phi^{\hbar}(Z + i\pi \hbar) - \phi^{\hbar}(Z - i\pi \hbar) &= \frac{2\pi i \hbar}{1 + e^{-Z}}, \\ \phi^{\hbar}(Z + i\pi) - \phi^{\hbar}(Z - i\pi) &= \frac{2\pi i}{1 + e^{-Z/\hbar}} \end{aligned}$$

and is meromorphic in the complex plane with the poles at the points $\{\pi i(m + n\hbar), m, n \in \mathbb{Z}_+\}$ and $\{-\pi i(m + n\hbar), m, n \in \mathbb{Z}_+\}$.

The function $\phi^{\hbar}(Z)$ is therefore holomorphic in the strip $|\operatorname{Im} Z| < \pi \min(1, \operatorname{Re} \hbar) - \epsilon$ for any $\epsilon > 0$, so we need only its asymptotic behavior as $Z \in \mathbb{R}$ and $|Z| \rightarrow \infty$, for which we have (see, e.g., [18])

$$\phi^{\hbar}(Z) \Big|_{|Z| \rightarrow \infty} = (Z + |Z|)/2 + O(1/|Z|). \quad (5.4)$$

We then have the following theorem ([5], [19])

Theorem 5.3 *The family of algebras $\mathcal{T}^{\hbar} = \mathcal{T}^{\hbar}(\Gamma_{g,\delta})$ is a quantization of $\mathcal{T}_{g,\delta}^H$ for any three-valent fatgraph spine $\Gamma_{g,\delta}$ of $\Sigma_{g,\delta}$, that is,*

- *In the limit $\hbar \mapsto 0$, morphism (3.2) using (5.3) coincides with classical morphism (3.2) with $\phi(Z) = \log(1 + e^Z)$.*
- *Morphism (3.2) using (5.3) is indeed a morphism of $*$ -algebras.*
- *A flip W_Z satisfies $W_Z^2 = I$.*
- *Flips on inner edges having exactly one common vertex satisfy the pentagon relation.*

5.3 Quantum geodesic functions

We next embed the algebra of geodesic functions (2.5) into a suitable completion of the constructed algebra \mathcal{T}^h . For any geodesic γ , the geodesic function G_γ can be expressed in terms of shear coordinates on \mathcal{T}^H :

$$G_\gamma \equiv \text{tr } P_{Z_1 \dots Z_n} = \sum_{j \in J} \exp \left\{ \frac{1}{2} \sum_{\alpha \in E(\Gamma)} m_j(\gamma, \alpha) Z_\alpha \right\}, \quad (5.5)$$

where $m_j(\gamma, \alpha)$ are integers and J is a finite set of indices.

In general, sets of integers $\{m_j(\gamma, \alpha)\}_{\alpha=1}^{6g-6+3s+2|\delta|}$ may coincide for different $j_1, j_2 \in J$; we however distinguish between them as soon as they come from different products of exponentials $e^{\pm Z_i/2}$ in traces of matrix products in (5.5).

For any closed path γ on $\Sigma_{g,\delta}$, define the *quantum geodesic* operator $G_\gamma^h \in \mathcal{T}^h$ to be

$$G_\gamma^h \equiv \times \text{tr } P_{Z_1 \dots Z_n} \times \equiv \sum_{j \in J} \exp \left\{ \frac{1}{2} \sum_{\alpha \in E(\Gamma_{g,\delta})} (m_j(\gamma, \alpha) Z_\alpha^h + 2\pi i \hbar c_j(\gamma, \alpha)) \right\}, \quad (5.6)$$

where the *quantum ordering* $\times \cdot \times$ implies that we vary the classical expression (5.5) by introducing additional integer coefficients $c_j(\gamma, \alpha)$, which must be determined from the conditions below.

That is, we assume that each term in the classical expression (5.5) can get multiplicative corrections only of the form q^n , $n \in \mathbb{Z}$, with

$$q \equiv e^{-i\pi\hbar}. \quad (5.7)$$

We now formulate the defining properties of quantum geodesics.

1. *Commutativity.* If closed paths γ and γ' do not intersect, then the operators G_γ^h and $G_{\gamma'}^h$ commute.
2. *Naturality.* The mapping class group (3.2) acts naturally on the set $\{G_\gamma^h\}$, i.e., for any transformation W^h from the mapping class groupoid and for a closed path γ in a spine $\Gamma_{g,\delta}$ of $\Sigma_{g,\delta}$, we have

$$W^h(G_\gamma^h) = G_{W(\gamma)}^h.$$
3. *Quantum geodesic algebra.* The product of two quantum geodesics is a linear combination of quantum multicurves governed by the (quantum) skein relation below.
4. *Orientation invariance.* As in the classical case, the quantum geodesic operator does not depend on the orientation of the corresponding geodesic line.
5. *Exponents of geodesics.* A quantum geodesic $G_{n\gamma}^h$ corresponding to the n -fold concatenation of γ is expressed via G_γ^h exactly as in the classical case, namely,

$$G_{n\gamma}^h = 2T_n(G_\gamma^h/2), \quad (5.8)$$

where $T_n(x)$ are Chebyshev's polynomials.

6. *Hermiticity.* A quantum geodesic is a Hermitian operator having by definition a real spectrum.

We let the standard normal ordering symbol $::$ denote the *Weyl ordering*, $:e^{a_1}e^{a_2}\dots e^{a_n}: \equiv e^{a_1+\dots+a_n}$, for any set of exponents with $a_i \neq -a_j$ for $i \neq j$.

Definition 5.1 For a spine $\Gamma_{g,\delta}$, we call a geodesic *graph simple* if it does not pass twice through any of inner edges of the graph and *undergoes at most one inversion* at any of the dot vertices.

Proposition 5.4 For any graph simple geodesic γ with respect to any spine Γ , the coefficients $c_j(\gamma, \alpha)$ in (5.6) are identically zero, i.e., the quantum ordering is the Weyl ordering.

5.4 Quantum skein relations

We now formulate the *general* rules that allow one to disentangle the product of any two quantum geodesics.

Let G_1^{\hbar} and G_2^{\hbar} be two quantum geodesic operators corresponding to geodesics γ_1 and γ_2 where all the inversion relations are resolved using the dot-vertex construction. Then

- We must apply the *quantum skein relation* ⁶

$$\begin{array}{c} G_1^{\hbar} \\ \diagdown \\ G_2^{\hbar} \end{array} \begin{array}{c} \diagup \\ \diagdown \end{array} = e^{-i\pi\hbar/2} \begin{array}{c} \text{)} \\ \text{(} \end{array} \begin{array}{c} \text{(} \\ \text{)} \end{array} + e^{i\pi\hbar/2} \begin{array}{c} \text{)} \\ \text{(} \end{array} \begin{array}{c} \text{(} \\ \text{)} \end{array} \quad (5.9)$$

simultaneously at *all* intersection points.

- After the application of the quantum skein relation we can obtain empty (contractible) loops; we assign the factor $-q - q^{-1}$ to each such loop and this suffices to ensure the quantum Reidemeister moves.
- We can also obtain loops that are homeomorphic to going around a dot-vertex; as in the classical case, we claim the corresponding geodesic functions to vanish, $\text{tr } F = 0$, so we erase all such cases of geodesic laminations in the quantum case as well.

The main lemma is in order.

Lemma 5.5 [5], [23] *There exists a unique quantum ordering $\times \dots \times$ (5.6), which is generated by the quantum geodesic algebra (5.9) and is consistent with the quantum transformations (3.2), i.e., so that the quantum geodesic algebra is invariant under the action of the quantum mapping class groupoid.*

⁶Here the order of crossing lines corresponding to G_1^{\hbar} and G_2^{\hbar} depends on which quantum geodesic occupies the first place in the product; the rest of the graph remains unchanged for all items in (5.9).

Example 5.1 For the pattern of the quantum geodesic functions in Fig. 10, we have (provided γ_1 and γ_2 have no more intersections)

$$G_1^{\hbar} \cdot G_2^{\hbar} = qG_U^{\hbar} + q^{-1}G_{\cap}^{\hbar} + G_{\supset}^{\hbar} \cdot G_C^{\hbar}.$$

This algebra simplifies further in the case where $G_1^{\hbar} = \times \text{tr } F_{i_1} F_j \times := G_{i_1, j}^{\hbar}$ and $G_2^{\hbar} = \times \text{tr } F_j F_{i_2} \times := G_{j, i_2}^{\hbar}$ with $i_1 < j < i_2$ because in this case $G_{\supset}^{\hbar} = \times \text{tr } F_{i_1} \times = 0$ and $G_C^{\hbar} = \times \text{tr } F_{i_2} \times = 0$. Then, taking into account that the product in the opposite order gives

$$G_2^{\hbar} \cdot G_1^{\hbar} = q^{-1}G_U^{\hbar} + qG_{\cap}^{\hbar} + G_{\supset}^{\hbar} \cdot G_C^{\hbar},$$

and that, for $G_1^{\hbar} = G_{i_1, j}^{\hbar}$ and $G_2^{\hbar} = G_{j, i_2}^{\hbar}$, $G_{\cap}^{\hbar} = \times \text{tr } F_{i_1} F_{i_2} \times := G_{i_1, i_2}^{\hbar}$ we obtain for the q -commutator

$$qG_{i_1, j}^{\hbar} \cdot G_{j, i_2}^{\hbar} - q^{-1}G_{j, i_2}^{\hbar} \cdot G_{i_1, j}^{\hbar} = (q^2 - q^{-2})G_{i_1, i_2}^{\hbar}.$$

This relation is among basic relations for the quantum Nelson–Regge algebras [21].

In Fig. 13, we present the quantum skein relation for quadruple intersection of geodesic functions (note that we must assign $-q - q^{-1}$ to every contractible loop).

5.5 Quantum braid group relation

5.5.1 Quantum A_n -algebra

We now consider the quantum geodesic functions associated with paths in the A_n -algebra pattern in Fig. 11.

We first generalize Example 5.1 to the case of general A_n algebras. For the quantum geodesic functions $G_{i, j}^{\hbar}$ ($i < j$) we have (assuming $j < i < l < k$)

$$\begin{aligned} [G_{ik}^{\hbar}, G_{jl}^{\hbar}] &= \xi \left(G_{jk}^{\hbar} G_{il}^{\hbar} - G_{ji}^{\hbar} G_{lk}^{\hbar} \right); \\ qG_{il}^{\hbar} G_{ji}^{\hbar} - q^{-1}G_{ji}^{\hbar} G_{il}^{\hbar} &= \xi G_{jl}^{\hbar}; \quad \xi = q^2 - q^{-2}. \\ qG_{jl}^{\hbar} G_{il}^{\hbar} - q^{-1}G_{il}^{\hbar} G_{jl}^{\hbar} &= \xi G_{ji}^{\hbar}; \end{aligned} \quad (5.10)$$

and, apparently, quantum geodesic functions corresponding to nonintersecting geodesics commute.

From the quantum skein relation, it is easy to obtain quantum transformations for $G_{i, j}^{\hbar}$. We introduce the \mathcal{A}^{\hbar} -matrix

$$\mathcal{A}^{\hbar} = \begin{pmatrix} q^{-1} & G_{1,2}^{\hbar} & G_{1,3}^{\hbar} & \cdots & G_{1,n}^{\hbar} \\ 0 & q^{-1} & G_{2,3}^{\hbar} & \cdots & G_{2,n}^{\hbar} \\ 0 & 0 & q^{-1} & \ddots & \vdots \\ \vdots & \vdots & \ddots & \ddots & G_{n-1,n}^{\hbar} \\ 0 & 0 & \cdots & 0 & q^{-1} \end{pmatrix} \quad (5.11)$$

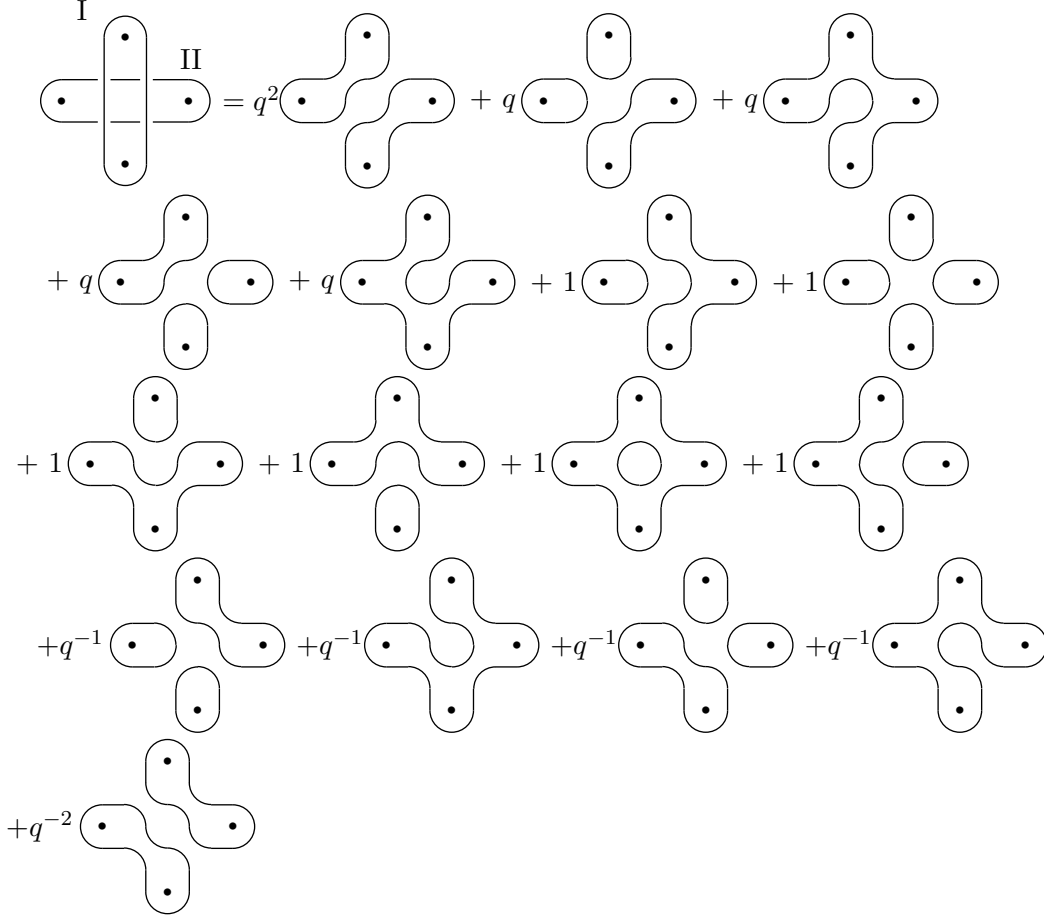


Figure 13: The quantum skein relation for the quantum geodesics functions G_{ij}^{\hbar} (indicated by I) and G_{kl}^{\hbar} (indicated by II) at $i < k < j < l$. Multicurves containing components homeomorphic to passing around the orbifold points vanish. Taking into account the symmetry w.r.t. changing the order of G_{ij} and G_{kl} in the product, we find that only the first (with q^2) and the last (with q^{-2}) terms contribute to the commutator.

associating the Hermitian operators $G_{i,j}^{\hbar}$ with the quantum geodesic functions. Using the skein relation, we can then present the action of the braid group element $R_{i,i+1}^{\hbar}$ exclusively in terms of the geodesic functions from this, fixed set: $R_{i,i+1}^{\hbar} \mathcal{A}^{\hbar} = \tilde{\mathcal{A}}^{\hbar}$, where

$$\begin{aligned}
\tilde{G}_{i+1,j}^{\hbar} &= G_{i,j}^{\hbar} & j > i + 1, \\
\tilde{G}_{j,i+1}^{\hbar} &= G_{j,i}^{\hbar} & j < i, \\
\tilde{G}_{i,j}^{\hbar} &= q^{-1} G_{i,j}^{\hbar} G_{i,i+1}^{\hbar} - q^{-2} G_{i+1,j}^{\hbar} = q G_{i,i+1}^{\hbar} G_{i,j}^{\hbar} - q^2 G_{i+1,j}^{\hbar} & j > i + 1, \cdot \\
\tilde{G}_{j,i}^{\hbar} &= q^{-1} G_{j,i}^{\hbar} G_{i,i+1}^{\hbar} - q^{-2} G_{j,i+1}^{\hbar} = q G_{i,i+1}^{\hbar} G_{j,i}^{\hbar} - q^2 G_{j,i+1}^{\hbar} & j < i, \\
\tilde{G}_{i,i+1}^{\hbar} &= G_{i,i+1}^{\hbar}
\end{aligned} \tag{5.12}$$

We can again present this transformation via the special matrices $B_{i,i+1}^{\hbar}$ of the block-

$$\begin{aligned}
\text{Case b} \quad & [G_{jl}^{\hbar}, G_{ii}^{\hbar}] = \xi \left(G_{ji}^{\hbar} G_{ll}^{\hbar} - G_{il}^{\hbar} G_{jj}^{\hbar} \right); \\
\text{Cases b}_{1,2} \quad & q G_{jj}^{\hbar} G_{kj}^{\hbar} - q^{-1} G_{kj}^{\hbar} G_{jj}^{\hbar} = \xi G_{kk}^{\hbar}, \quad q G_{jk}^{\hbar} G_{jj}^{\hbar} - q^{-1} G_{jj}^{\hbar} G_{jk}^{\hbar} = \xi G_{kk}^{\hbar}; \\
\text{Case c} \quad & [G_{ii}^{\hbar}, G_{kk}^{\hbar}] = (q - q^{-1})(G_{ik}^{\hbar} - G_{ki}^{\hbar}). \tag{5.17} \\
\text{Case d} \quad & [G_{ij}^{\hbar}, G_{kl}^{\hbar}] = \xi \left(G_{kj}^{\hbar} G_{li}^{\hbar} - G_{jk}^{\hbar} G_{il}^{\hbar} + G_{jl}^{\hbar} G_{ik}^{\hbar} - G_{lj}^{\hbar} G_{ki}^{\hbar} \right. \\
& \quad \left. + (q + q^{-1})(G_{il}^{\hbar} G_{jj}^{\hbar} G_{kk}^{\hbar} - G_{kj}^{\hbar} G_{ll}^{\hbar} G_{ii}^{\hbar}) \right); \\
\text{Case d}_1 \quad & q G_{jl}^{\hbar} G_{ij}^{\hbar} - q^{-1} G_{ij}^{\hbar} G_{jl}^{\hbar} = \xi \left(q^{-1} G_{lj}^{\hbar} G_{ji}^{\hbar} + q G_{ii}^{\hbar} G_{ll}^{\hbar} + q^{-1} G_{ll}^{\hbar} G_{ii}^{\hbar} \right. \\
& \quad \left. - q^{-2} G_{li}^{\hbar} - G_{il}^{\hbar} (G_{jj}^{\hbar})^2 \right); \\
\text{Case d}_2 \quad & [G_{jl}^{\hbar}, G_{lj}^{\hbar}] = \xi \left((G_{ll}^{\hbar})^2 - (G_{jj}^{\hbar})^2 \right);
\end{aligned}$$

Although these relations contain not only triple terms in the r.h.s. but also noncommuting terms (this is the price for closing the algebra), they nevertheless establish the lexicographic ordering on the corresponding set of quantum variables $\{G_{ij}^{\hbar}\}$.

Lemma 5.7 *Permutation relations postulated by (5.17) satisfy the (quantum) Jacobi identities.*

The proof is tedious but straightforward calculations. Note that algebra (5.17) is consistent even without relation to geometry of modular spaces; the similar phenomenon was already observed in the case of A_n -algebras.

We now provide the quantum version of the braid group transformations (4.22) and (4.23). For $R_{i,i+1}^{\hbar}$ with $1 \leq i \leq n-1$, we have

$$\begin{aligned}
\tilde{G}_{i+1,k}^{\hbar} &= G_{i,k}^{\hbar} & k \neq i, i+1, \\
\tilde{G}_{i,k}^{\hbar} &= q G_{i,i+1}^{\hbar} G_{i,k}^{\hbar} - q^2 G_{i+1,k}^{\hbar} = q^{-1} G_{i,k}^{\hbar} G_{i,i+1}^{\hbar} - q^{-2} G_{i+1,k}^{\hbar} & k \neq i, i+1, \\
\tilde{G}_{k,i+1}^{\hbar} &= G_{k,i}^{\hbar} & k \neq i, i+1, \\
\tilde{G}_{k,i}^{\hbar} &= q G_{i,i+1}^{\hbar} G_{k,i}^{\hbar} - q^2 G_{k,i+1}^{\hbar} = q^{-1} G_{k,i}^{\hbar} G_{i,i+1}^{\hbar} - q^{-2} G_{k,i+1}^{\hbar} & k \neq i, i+1, \\
\tilde{G}_{i,i+1}^{\hbar} &= G_{i,i+1}^{\hbar}, \\
\tilde{G}_{i+1,i+1}^{\hbar} &= G_{i,i}^{\hbar}, \\
\tilde{G}_{i,i}^{\hbar} &= q G_{i,i+1}^{\hbar} G_{i,i}^{\hbar} - q^2 G_{i+1,i+1}^{\hbar} = q^{-1} G_{i,i}^{\hbar} G_{i,i+1}^{\hbar} - q^{-2} G_{i+1,i+1}^{\hbar}, \\
\tilde{G}_{i+1,i}^{\hbar} &= G_{i+1,i}^{\hbar} + G_{i,i}^{\hbar} G_{i,i+1}^{\hbar} G_{i,i}^{\hbar} - q^{-1} G_{i+1,i+1}^{\hbar} G_{i,i}^{\hbar} - q G_{i,i}^{\hbar} G_{i+1,i+1}^{\hbar},
\end{aligned} \tag{5.18}$$

and for $R_{n,1}^h$, we have

$$\begin{aligned}
\tilde{G}_{1,k}^h &= G_{n,k}^h & k \neq n, 1, \\
\tilde{G}_{n,k}^h &= qG_{n,1}^h G_{n,k}^h - q^2 G_{1,k}^h = q^{-1} G_{n,k}^h G_{n,1}^h - q^{-2} G_{1,k}^h & k \neq n, 1, \\
\tilde{G}_{k,1}^h &= G_{k,n}^h & k \neq n, 1, \\
\tilde{G}_{k,n}^h &= qG_{n,1}^h G_{k,n}^h - q^2 G_{k,1}^h = q^{-1} G_{k,n}^h G_{n,1}^h - q^{-2} G_{k,1}^h & k \neq n, 1, \\
\tilde{G}_{n,1}^h &= G_{n,1}^h, \\
\tilde{G}_{1,1}^h &= G_{n,n}^h, \\
\tilde{G}_{n,n}^h &= qG_{n,1}^h G_{n,n}^h - q^2 G_{1,1}^h = q^{-1} G_{n,n}^h G_{n,1}^h - q^{-2} G_{1,1}^h, \\
\tilde{G}_{1,n}^h &= G_{1,n}^h + G_{n,n}^h G_{n,1}^h G_{n,n}^h - q^{-1} G_{1,1}^h G_{n,n}^h - q G_{n,n}^h G_{1,1}^h,
\end{aligned} \tag{5.19}$$

Lemma 5.8 *For any $n \geq 3$, we have the quantum braid group relations*

$$R_{i-1,i}^h R_{i,i+1}^h R_{i-1,i}^h = R_{i,i+1}^h R_{i-1,i}^h R_{i,i+1}^h, \quad i = 1, \dots, n \text{ mod } n \tag{5.20}$$

for transformations (5.18), (5.19) of quantum operators subject to quantum algebra (5.17).

Again, the second identity (5.16) is lost in the case of D_n algebras.

5.5.3 Matrix representation for D_n -algebra and invariants

We now construct the quantum version of Theorem 4.6. For this, we first need a preparatory lemma.

Lemma 5.9 *The following four matrices with operatorial entries, together with all their linear combinations, transform in accordance with the quantum braid-group action (5.14): \mathcal{A}^h (5.11), $(\mathcal{A}^h)^\dagger$, \mathcal{R}^h , and \mathcal{S}^h , where*

$$(\mathcal{R}^h)_{i,j} = \begin{cases} -G_{j,i}^h - q^2 G_{i,j}^h + q G_{i,i}^h G_{j,j}^h & j > i \\ G_{i,j}^h + q^{-2} G_{j,i}^h - q^{-1} G_{i,i}^h G_{j,j}^h & j < i \\ 0 & j = i \end{cases} ; \quad (\mathcal{R}^h)^\dagger = -\mathcal{R}^h, \tag{5.21}$$

$$(\mathcal{S}^h)_{i,j} = G_{i,i}^h G_{j,j}^h \text{ for all } 1 \leq i, j \leq n, \quad (\mathcal{S}^h)^\dagger = \mathcal{S}^h. \tag{5.22}$$

The quantum $(4n) \times (4n)$ matrix $\mathbb{B}_{i,i+1}^h$ for $1 \leq i \leq n-1$ has the block-diagonal form (4.28) with diagonal entries being $n \times n$ -matrices $B_{i,i+1}^h$ (5.13), whereas the remaining

matrix $\mathbb{B}_{n,1}^{\hbar}(\lambda)$ reads

$$\mathbb{B}_{n,1}^{\hbar}(\lambda) = \begin{pmatrix} 0 & & & & \lambda^2 \\ & \mathcal{I} & & & \\ & qG_{1,n}^{\hbar} & -q^2 & & \\ \hline & 1 & 0 & & \\ & & \mathcal{I} & & \\ & & qG_{1,n}^{\hbar} & -q^2 & \\ \hline & & 1 & 0 & \\ & & & \mathcal{I} & \\ & & & qG_{1,n}^{\hbar} & -q^2 \\ \hline & & & 1 & 0 \\ & & & & \mathcal{I} \\ -\lambda^{-2}q^2 & & & & qG_{1,n}^{\hbar} \end{pmatrix}, \quad (5.23)$$

and introducing the quantum matrix

$$\mathbb{A}^{\hbar} = \begin{bmatrix} \mathcal{A}^{\hbar} & B^{\hbar} & C^{\hbar} & (B^{\hbar})^{\dagger} \\ 0 & \mathcal{A}^{\hbar} & B^{\hbar} & C^{\hbar} \\ 0 & 0 & \mathcal{A}^{\hbar} & B^{\hbar} \\ 0 & 0 & 0 & \mathcal{A}^{\hbar} \end{bmatrix}, \quad \text{where } \begin{cases} B^{\hbar} = \mathcal{R}^{\hbar} + q^{-1}\mathcal{S}^{\hbar} + q^2\mathcal{A}^{\hbar} - q^{-2}(\mathcal{A}^{\hbar})^{\dagger}, \\ C^{\hbar} = (q + q^{-1})\mathcal{S}^{\hbar} - \mathcal{A}^{\hbar} - (\mathcal{A}^{\hbar})^{\dagger}, \end{cases}, \quad (5.24)$$

we come to the main theorem about quantum braid-group representation.

Theorem 5.10 *The quantum braid group relations (5.18) and (5.19) can be presented in the form of matrix relations for the matrix $\lambda\mathbb{A}^{\hbar} + \lambda^{-1}(\mathbb{A}^{\hbar})^{\dagger}$ with the matrix \mathbb{A}^{\hbar} defined in (5.24):*

$$R_{i,i+1}^{\hbar}(\lambda\mathbb{A}^{\hbar} + \lambda^{-1}(\mathbb{A}^{\hbar})^{\dagger}) = \mathbb{B}_{i,i+1}^{\hbar}(\lambda\mathbb{A}^{\hbar} + \lambda^{-1}(\mathbb{A}^{\hbar})^{\dagger})(\mathbb{B}_{i,i+1}^{\hbar})^{\dagger}, \quad i = 1, \dots, n - (5.25)$$

$$R_{n,1}^{\hbar}(\lambda\mathbb{A}^{\hbar} + \lambda^{-1}(\mathbb{A}^{\hbar})^{\dagger}) = \mathbb{B}_{n,1}^{\hbar}(\lambda)(\lambda\mathbb{A}^{\hbar} + \lambda^{-1}(\mathbb{A}^{\hbar})^{\dagger})(\mathbb{B}_{n,1}^{\hbar}(\lambda^{-1}))^{\dagger}, \quad (5.26)$$

where $\mathbb{B}_{i,i+1}^{\hbar}$ has the form (4.28) with $B_{i,i+1}$ replaced by $B_{i,i+1}^{\hbar}$ from (5.13) and with $\mathbb{B}_{n,1}^{\hbar}(\lambda)$ of the form (5.23).

Example 5.2 In the case $n = 2$, the combination

$$G_{1,1}^{\hbar}G_{2,2}^{\hbar} - qG_{1,2}^{\hbar} - q^{-1}G_{2,1}^{\hbar} = G_{2,2}^{\hbar}G_{1,1}^{\hbar} - q^{-1}G_{1,2}^{\hbar} - qG_{2,1}^{\hbar}$$

is a central element of the (quantum) algebra D_2 ; the other central element is

$$G_{1,2}^{\hbar}G_{2,1}^{\hbar} - q^2(G_{2,2}^{\hbar})^2 - q^{-2}(G_{1,1}^{\hbar})^2 = G_{2,1}^{\hbar}G_{1,2}^{\hbar} - q^{-2}(G_{2,2}^{\hbar})^2 - q^2(G_{1,1}^{\hbar})^2.$$

Example 5.3 A cyclic permutation of indices $P : i \mapsto i + 1 \bmod n; j \mapsto j + 1 \bmod n$ destroys the structure of the matrix \mathcal{A}^h and results in the following transformations for \mathcal{R}^h and \mathcal{S}^h :

$$P : \mathcal{R}^h \mapsto \begin{pmatrix} 0 & 1 & & \\ & \ddots & \ddots & \\ & & \ddots & 1 \\ -q^{-2} & & & 0 \end{pmatrix} \mathcal{R}^h \begin{pmatrix} 0 & & -q^2 \\ 1 & \ddots & \\ & \ddots & \ddots \\ & & 1 & 0 \end{pmatrix}, \quad (5.27)$$

$$P : \mathcal{S}^h \mapsto \begin{pmatrix} 0 & 1 & & \\ & \ddots & \ddots & \\ & & \ddots & 1 \\ 1 & & & 0 \end{pmatrix} \mathcal{S}^h \begin{pmatrix} 0 & & 1 \\ 1 & \ddots & \\ & \ddots & \ddots \\ & & 1 & 0 \end{pmatrix}. \quad (5.28)$$

These transformations together with (5.14) must also generate a full modular group. From this, we find that $\det \mathcal{R}$ must be itself the mapping-class group invariant lying therefore in the center of the Poisson algebra. Same is true for \mathcal{S} , but $\det \mathcal{S} \equiv 0$ whereas $\det \mathcal{R}$ is nonzero for even $n = 2m$ (and vanishes for odd n): denoting $Q_{i,j} := (\mathcal{R})_{i,j}$ for $i < j$, we have $\det \mathcal{R} = \text{Pf}_{2m}^2$, where the Pfaffian Pf_{2m} is given by the parity-signed sum over all possible pairings in the set of indices $1, 2, \dots, 2m - 1, 2m$.

For example, for $m = 2$, we have

$$\text{Pf}_4 = Q_{1,2}Q_{3,4} + Q_{1,4}Q_{2,3} - Q_{1,3}Q_{2,4}$$

(recall that $Q_{i,j} = G_{i,j} + G_{j,i} - G_{i,i}G_{j,j}$ in the classical case). In the quantum case, these elements acquire q -corrections.

Acknowledgments

The author acknowledges useful discussions with V. V. Fock, S. Fomin, M. Mazzocco, S. N. Natanzon, R. C. Penner, M. Shapiro, and D. Thurston. The author thanks the referee for the useful remarks and for the careful reading of the manuscript.

The work was partially financially supported by the Russian Foundation for Basic Research (Grant Nos. 06-02-17383 and 09-01-92433-CE), Grants of Support for the Scientific Schools 795.2008.1, by the Program Mathematical Methods of Nonlinear Dynamics, by the European Community through the FP6 Marie Curie RTN *ENIGMA* (Contract number MRTN-CT-2004-5652), and by EPSRC Grant EP/D071895/1.

References

- [1] F. Bonahon, *Shearing hyperbolic surfaces, bending pleated surfaces and Thurston's symplectic form*, *Ann. Fac. Sci. Toulouse Math* 6 **5** (1996), 233-297.

- [2] A. Bondal, *A symplectic groupoid of triangular bilinear forms and the braid groups*, preprint IHES/M/00/02 (Jan. 2000).
- [3] L. O. Chekhov, *Teichmüller theory of bordered surfaces*, SIGMA Symmetry Integrability Geom. Methods Appl. **3** (2007), Paper 066, 37pp. (electronic)
- [4] L. O. Chekhov, *Riemann surfaces with orbifold points*, to appear in *Proc. Steklov Math. Inst.* (2009).
- [5] L. Chekhov and V. Fock, talk on May, 25 at *St. Petersburg Meeting on Selected Topics in Mathematical Physics*, LOMI, 26–29 May, 1997; *A quantum Teichmüller space*, *Theor. Math. Phys.*, **120** (1999) 1245–1259; *Quantum mapping class group, pentagon relation, and geodesics* *Proc. Steklov Math. Inst.* **226** (1999) 149–163.
- [6] L. O. Chekhov and V. V. Fock, *Observables in 3d gravity and geodesic algebras*, *Czech. J. Phys.* **50** (2000) 1201–1208.
- [7] L. O. Chekhov and M. Mazzocco, *New Poisson algebras arising in Teichmüller theory*, in preparation.
- [8] L.O. Chekhov and R.C. Penner, *On quantizing Teichmüller and Thurston theories*, Chapter 14 in: *Handbook on Teichmüller Theory*, Vol.1 (IRMA Lectures in Mathematics and Physics, Vol.11), ed. A.Papadopoulos, IRMA Publ., Strasbourg, France. pp.579-646; math.AG/0403247.
- [9] B. A. Dubrovin and M. Mazzocco, *Monodromy of certain Painlevé-VI transcendents and reflection group*, *Invent. Math.* **141** (2000) 55–147.
- [10] J. J. Etayo and E. Martínez, *Fuchsian groups generated by half-turns and geometrical characterization of hyperelliptic and symmetric Riemann surfaces*, *Math. Scand.* **95** (2004) 226–244.
- [11] L. D. Faddeev, *Discrete Heisenberg–Weyl group and modular group*, *Lett. Math. Phys.*, **34**, (1995), 249–254.
- [12] V. V. Fock, *Combinatorial description of the moduli space of projective structures*, hep-th/9312193.
- [13] V. V. Fock, *Dual Teichmüller spaces*, dg-ga/9702018.
- [14] V. V. Fock and A. B. Goncharov, *Dual Teichmüller and lamination spaces*, Chapter 15 in: *Handbook on Teichmüller Theory*, Vol.1 (IRMA Lectures in Mathematics and Physics, Vol.11), ed. A.Papadopoulos, IRMA Publ., Strasbourg, France. pp.647-684; math.DG/0510312.
- [15] S. Fomin, M. Shapiro, and D. Thurston, *Cluster algebras and triangulated surfaces. Part I: Cluster complexes*, math.RA/0608367.
- [16] S. Fomin and A. Zelevinsky, *Cluster algebras I: Foundations*, *J. Amer. Math. Soc.* **15**(2) (2002) 497–529; *The Laurent phenomenon*, math.CO/0104241.

- [17] W. M. Goldman, *Invariant functions on Lie groups and Hamiltonian flows of surface group representations*, *Invent. Math.*, **85**, (1986), 263–302.
- [18] R. M. Kashaev, *On the spectrum of Dehn twists in quantum Teichmüller theory*, in: *Physics and Combinatorics*, (Nagoya 2000). River Edge, NJ, World Sci. Publ., 2001, 63–81; math.QA/0008148.
- [19] R. M. Kashaev, *Quantization of Teichmüller spaces and the quantum dilogarithm*, *Lett. Math. Phys.*, **43**, No. 2, (1998), 105–115; q-alg/9705021.
- [20] R. M. Kaufmann and R. C. Penner, *Closed/open string diagrammatics*, *Nucl. Phys.* **B748** (2006) 335–379.
- [21] J. E. Nelson and T. Regge, *2+1 quantum gravity*, *Phys. Lett.* **B272**, (1991), 213–216; J. E. Nelson and T. Regge, *Invariants of 2 + 1 gravity*, *Commun. Math. Phys.* **155**, (1993) 561–568.
- [22] R. C. Penner, *The decorated Teichmüller space of Riemann surfaces*, *Commun. Math. Phys.*, **113**, (1988), 299–339.
- [23] J. Teschner, *An analog of a modular functor from quantized Teichmüller theory*, math.QA/0510174.
- [24] W. P. Thurston, *Minimal stretch maps between hyperbolic surfaces*, preprint (1984), math.GT/9801039.
- [25] M. Ugaglia: *On a Poisson structure on the space of Stokes matrices*, *Int. Math. Res. Not.*, **1999**, No. 9, (1999), 473–493; math.ag/9902045.